CHEMMEDCHEM

CHEMISTRY ENABLING DRUG DISCOVERY

Accepted Article

Title: Development of Potent Inhibitors of Fatty Acid Amide Hydrolase Useful for the Treatment of Neuropathic Pain

Authors: Margherita Brindisi, Giuseppe Borrelli, Simone Brogi, Alessandro Grillo, Samuele Maramai, Marco Paolino, Mascia Benedusi, Alessandra Pecorelli, Giuseppe Valacchi, Lorenzo Di Cesare Mannelli, Carla Ghelardini, Marco Allarà, Alessia Ligresti, Patrizia Minetti, Giuseppe Campiani, Stefania Butini, Vincenzo di Marzo, and Sandra Gemma

To be cited as: *ChemMedChem* 10.1002/cmdc.201800397

Link to VoR: http://dx.doi.org/10.1002/cmdc.201800397

A Journal of

ChemPubSoc Europe

WILEY-VCH

www.chemmedchem.org

WILEY-VCH

FULL PAPER

Development of Potent Inhibitors of Fatty Acid Amide Hydrolase Useful for the Treatment of Neuropathic Pain

Margherita Brindisi,[a] Giuseppe Borrelli,[†,a] Simone Brogi,[†,a] Alessandro Grillo,[†,a] Samuele Maramai,[†,a] Marco Paolino,[a] Mascia Benedusi,[b] Alessanda Pecorelli,[c] Giuseppe Valacchi,[b],[c] Lorenzo Di Cesare Mannelli,[d] Carla Ghelardini,[d] Marco Allarà,[e],[f] Alessia Ligresti,[e] Patrizia Minetti,[g] Giuseppe Campiani,[a]* Vincenzo di Marzo,[e],[h] Stefania Butini,[a]* Sandra Gemma[a]

[a] Dr. Margherita Brindisi, Dr. Giuseppe Borrelli, Dr. Simone Brogi, Dr. Alessandro Grillo, Dr. Samuele Maramai, Dr. Marco Paolino, Prof. Giuseppe Campiani, Prof. Stefania Butini, Prof. Sandra Gemma
European Research Centre for Drug Discovery and Development (NatSynDrugs) and Department of Biotechnology, Chemistry, and Pharmacy (DoE 2018-2020)
University of Siena
Via Aldo Moro 2, 53100 Siena, Italy
E-mail: : butini3@unisi.it; campiani@unisi.it
†These authors contributed equally

[b] Prof. Giuseppe Valacchi; Dr. Mascia Benedusi
Department of Life Sciences and Biotechnology
University of Ferrara
Via Borsari 46, 441212, Ferrara, Italy

[c] Prof. Giuseppe Valacchi, Dr. Alessanda Pecorelli
Department of Animal Science
North Carolina State University
NC Research Campus, PHHI Building, 600 Laureate Way, Kannapolis 28081, NC USA

[d] Prof. Carla Ghelardini, Dr. Lorenzo Di Cesare Mannelli
Department of Neuroscience, Psychology, Drug Research and Child Health, Section of Pharmacology and Toxicology (NEUROFARBA)
University of Florence
Viale G. Pieraccini, 6, 50139 Firenze, Italy

[e] Prof. Vincenzo di Marzo, Dr. Alessia Ligresti, Dr. Marco Allarà
Endocannabinoid Research Group, Institute of Biomolecular Chemistry
CNR
Via Campi Flegrei, 80078 Pozzuoli (Napoli), Italy

[f] Dr. Marco Allarà
EPITECH Group SpA
Via Egadi, 7 - 20144 Milano Italy

[g] Dr. Patrizia Minetti
Alfasigma
Via Pontina Km 30,400, 00040 Pomezia, Italy

[h] Prof. Vincenzo di Marzo
Département de Médecine
Université Laval
1050, avenue de la Médecine, Québec City (Québec), QC G1V 0A6, Canada

Supporting information for this article is given via a link at the end of the document.

Abstract. The unique role of fatty acid amide hydrolase (FAAH) in terminating endocannabinoid (EC) signaling supports its relevance as therapeutic target. Inhibition of the ECs metabolizing enzymes elicits indirect agonism of cannabinoid receptors (CBRs), and therapeutic efficacy, devoid of psychotropic effects. Based on our previous ligands and aiming at discovering new selective FAAH inhibitors, we developed a series of new compounds (**5a-l**) characterized by functionalized tricyclic scaffolds. All the developed compounds display negligible activity on MAGL and CBRs. The most potent FAAH inhibitors of the newly developed series, **5h** and **5i** (nanomaolar FAAH inhibitor also some detecting micromolar affinity at CB_1R), were selected for further studies. After cellular studies on a neuroblastoma cell line (IMR32) **5h,i** and our reference compound **3** demonstrated the lack of any cytotoxic effect and the ability to reduce oxidative stress by decreasing the expression of the redox sensitive transcription factor NF-kB. Encouraged by these data, compounds were studied *in vivo* and were dosed orally in a mice model of neuropathic pain. At 10 mg/kg all the compounds were able to relieve the hypersensitivity induced by oxaliplatin.

Introduction

Fatty acid amide hydrolase (FAAH, EC 3.5.1.99), an integral membrane-bound serine hydrolase,[1-2] is the main catabolic enzyme of the fatty acid ethanolamides (FAEs) such as anandamide (AEA) and oleamide.[3] Other enzymes that contribute to the termination of the endocannabinoids' (EC) action are N-acylethanolamine acid amidase[4] and monoacylglycerol lipase (MAGL).[5] FAEs together with 2-arachidonoylglycerol are the main EC signalling lipids which, by interacting with type-1 and type-2 cannabinoid receptors (CB_1R and CB_2R), exert biological activity and modulate a variety of physiological processes including pain, inflammation, appetite, motility, sleep, thermoregulation, cognition and emotional states.[6-7] The analgesic effect of CB_1R and CB_2R has been known for centuries[8] but, as other CBRs agonists, they produce a spectrum of motor and psychotropic side effects mediated by central CB_1R. Accordingly, a valuable therapeutic alternative aims at eliciting the desirable effects of CBRs activation, while avoiding the negative effects of global CB_1R stimulation, through indirect receptor agonism obtained by inactivation of ECBs metabolizing enzymes. The relevance of FAAH enzyme in the safe management of pain is supported by the evidence that *faah* knockout mice display high

AEA levels in central nervous system (CNS) and show an analgesic phenotype, in either models of inflammatory pain (induced by carrageenan) and of acute pain (induced by formalin,[9] together with a reduction of the inflammatory responses,[10] and improved sleep and memory acquisition,[11-12] supports the relevance of FAAH enzyme in the safe management of pain. In fact, FAAH inhibition by increasing the endogenous concentration of its substrates, protracts and potentiates their beneficial (therapeutic) effects, without eliciting the classical CB_1R agonist side effects (hypomotility, hypothermia, and catalepsy).[13] In 2016, the serious adverse effects observed in a phase I study with a FAAH irreversible inhibitor (BIA 10-2474) led to a temporary suspension of the development of FAAH inhibitors. Shortly after, a report from FDA[14] concluded that BIA 10-2474 has a peculiar toxicity profile that does not extend to other FAAH inhibitors. In fact, an in depth re-investigation uncovered a series of off-target proteins for the same compound.[15]

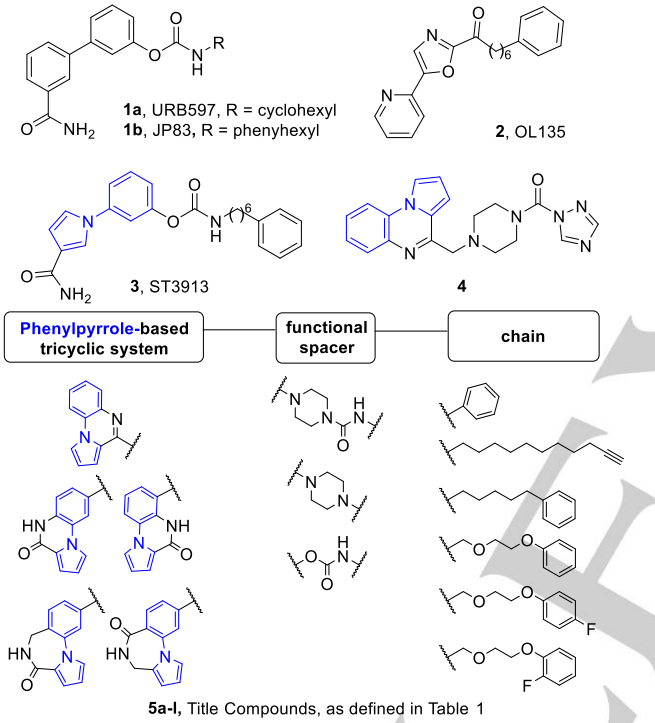

Figure 1. Reference (**1-4**) and title compounds (**5a-l**).

Chronic pain is a major public health problem, with a tremendous impact on the quality of life of the patients, that produces a significant economic and social burden.[16] Neuropathic pain (a severe, debilitating, and persistent, form of chronic pain that may arise from a dysfunction or damaged peripheral nerves, spinal cord, or brain[17]) is poorly treated by conventional therapeutics which also exhibit a series of drawbacks and side effects. All the above considerations suggest that the use of FAAH inhibitors may provide a safe and efficient approach for the treatment of painful syndromes including neuropathies.[17]

The crystal structure of FAAH enabled an in-depth knowledge of the enzyme features and functioning useful for the development of selective inhibitors. The catalytic triad (S241, S217, and K142, human numbering) is accessible through the acyl-binding channel and the "membrane access channel".[18] In proximity of the nucleophilic S241, the oxyanion hole accommodates the carbonyl oxygen of amide or ester substrates by establishing H-bonds. The different FAAH inhibitors developed so far, can be clustered in two families: irreversible (e.g. carbamates **1a**[19] and **1b**,[20] Figure 1) and reversible inhibitors (e.g. the α-ketooxazole **2**,[21] Figure 1). In this frame, we recently reported the development of different classes of compounds as inhibitors of the ECs metabolic enzymes; potent and selective FAAH[22-23] or MAGL[24] inhibitors and dual FAAH/MAGL[25] inhibitors useful in different pathological states.[26-27]

As a continuation of our efforts in the discovery of FAAH inhibitors we herein describe the development of pyrrole-based analogues inspired to our previously identified ligands. This new series of compounds (**5a-l**, Figure 1 and Table 1) our structural template, compound **3**, was modified in a classical medicinal chemistry approach which involved a structural rigidification by bridging the phenylpyrrole scaffold of our lead **3**. In particular three types of tricyclic systems were explored: i) a 6-6-5 system, the pyrrolo[1,2-*a*]quinoxaline (also inspired to the structure of previously developed FAAH/MAGL inhibitors typified by **4**[25]); ii) a 6-6-5 system, pyrrolo[1,2-*a*]quinoxalin-4(5*H*)-one substituted at C-6 or C-8; iii) the 6-7-5 systems 4,5-dihydro-6*H*-benzo[*f*]pyrrolo[1,2-*a*][1,4]diazepin-6-one and 5,6-dihydro-4*H*-benzo[*f*]pyrrolo[1,2-*a*][1,4]diazepin-4-one heterocycles, substituted at C-9. These systems were tethered by a piperazinyl urea or a carbamate to phenylhexyl, undecynyl, or ((monofluoro)phenoxyethoxyethyl lateral chains (Figure 1 and Table 1). Synthesis, molecular modelling, *in vitro* and *in vivo* biological properties of the new FAAH inhibitors are discussed in the present article.

Results and Discussion

Chemistry

The synthesis of compounds **5a−l** is described in Schemes 1−5. Reaction of pyrroloquinoxalyl intermediate **6**[28-31] (Scheme 1) with the alkylisocyanates **7a-c** afforded the piperazinecarboxamide-based compounds **5a−c**, whereas reaction with the alkyl bromides afforded the alkylpiperazine-based derivatives **5d,e**.[32]

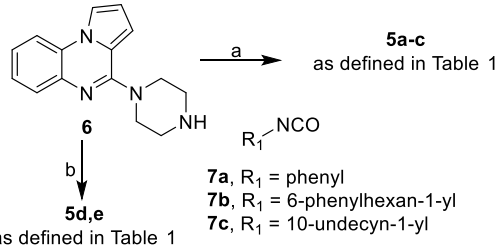

Scheme 1. Reagents and conditions: a) R_1NCO, TEA, dry THF, reflux, 11 h, 59-62%; b) R_2Br, TEA, MeCN, reflux, 14 h, 71-75%.

For the synthesis of **5f** (Scheme 2) the application of Curtius rearrangement protocol to the acid **8** with *tert*-butanol provided the protected aniline **9**. After Boc-removal, the amine **10** was converted, by a Clauson-Kaas reaction obtained, in turn converted into the 1-phenylpyrrole derivative **11**. Reduction of the nitro functionality led to amine **12** that by treatment with triphosgene provided the quinoxalinone **13**. Treatment with boron tribromide afforded the phenol **14** that was reacted with phenylhexylisocianate (**7b**) to achieve **5f**.

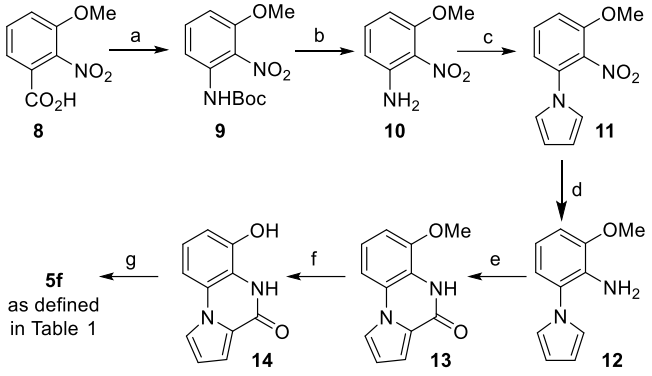

Scheme 2. Reagents and conditions: a) *t*-BuOH, DPPA, TEA, reflux, 15 h, 78%; b) TFA, 0 °C, 1.5 h, 99%; c) 2,5-dimethoxytetrahydrofuran, AcOH, H_2O, 100 °C, 15 min, 97%; d) Fe°, $CaCl_2$, EtOH 75%, 80 °C, 2 h, 87%; e) $CO(OCCl_3)_2$, toluene, 120 °C, 2 h, 52%; f) BBr_3, DCM, from-78 to 25 °C, 12 h, 11%; g) **7b**, TEA, THF, 25 °C, 16 h, 30%.

Nitration of the 3-hydroxyphenylacetamide **15** (Scheme 3) led to **16**. Sequential hydrolysis of the acetamido group, Clauson-Kaas reaction and reduction of the nitro functionality provided the aminophenol **17**. Cyclization reaction carried on with triphogene afforded derivative **18**, later converted into the urethane **5g**.

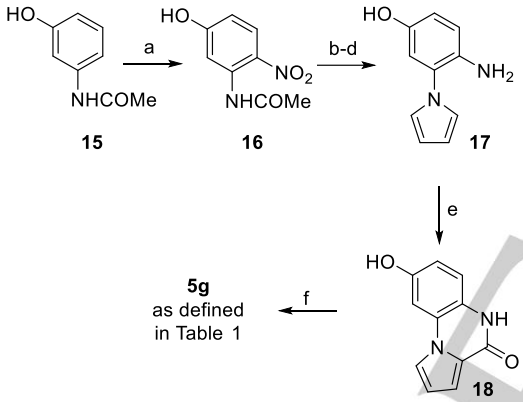

Scheme 3. Reagents and conditions: a) HNO_3, AcOH, Ac_2O, 25 °C, 8 h, 98%; b) 12N HCl, 130 °C, 5 h, 95%; c) 5N HCl, 2,5-dimethoxytetrahydrofuran, 1,4-dioxane, 110 °C, 20 min, 70%; d) $SnCl_2{\cdot}2H_2O$, EtOAc, 25 °C, 2 h, 85%; e) $CO(OCCl_3)_2$, toluene, 120 °C, 2 h, 36%; f) **7b**, TEA, THF, 25 °C, 16 h, 10%.

After esterification and nitro group reduction of the nitrocarboxylic acid **19** (Scheme 4) the resulting aniline was subjected to Clauson-Kaas reaction, to give the intermediate **20**. This 1-phenylpyrrole was converted into the 2-cyanopyrrole derivative **21**. Selective reduction of the nitrile by treatment with sodium borohydride in the presence of cobalt(II) chloride led to spontaneous cyclization to the pyrrolobenzo[1,4]diazepinone derivative **22**. Cleavage of the methyl ether functionality followed by treatment with phenylhexylisocianate provided **5h**.

For the preparation of compounds **5i-l** (Scheme 5) aryl fluoride **23** was submitted to an aromatic nucleophilic substitution with methyl 1*H*-pyrrole-2-carboxylate in the presence of cesium carbonate. The resulting 1-phenylpyrrole **24** was reduced, cyclized and treated with boron tribromide, thus providing the pyrrolobenzo[1,4]diazepinone intermediate **25**. Reaction with the isocyanates **7b** or **26a-c**[22] led to compounds **5i-l**.

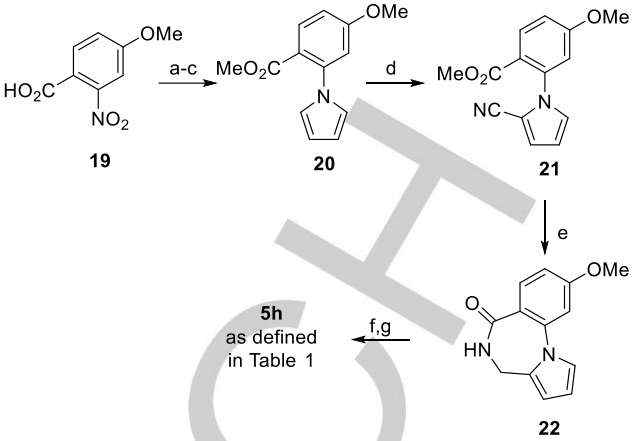

Scheme 4. Reagents and conditions: a) $SOCl_2$, MeOH, 25 °C, 10 h; b) $SnCl_2{\cdot}2H_2O$, EtOAc, 25 °C, 2 h; c) 5N HCl, 2,5-dimethoxytetrahydrofuran, 1,4-dioxane, 110 °C, 5 min, 87% (over 3 steps); d) $(COCl)_2$, $NH_2OH{\cdot}HCl$, pyridine, DMF, 1,2-DCE, from 0 to 120 °C, 10 h, 47%; e) $NaBH_4$, $CoCl_2$, MeOH, 25 °C, 30 min, 64%; f) BBr_3, DCM, from -78 to 25 °C, 12 h, 50%; g) **7b**, TEA, THF, 25 °C, 16 h, 60%.

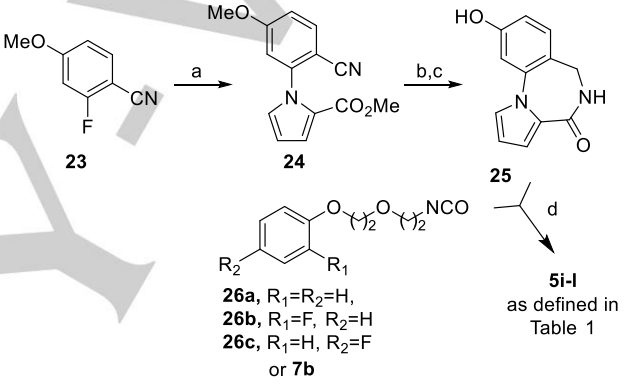

Scheme 5. Reagents and conditions: a) methyl 1*H*-pyrrole-2-carboxylate, Cs_2CO_3, dry DMF, 50 °C, 12 h, 30%; b) $NaBH_4$, $CoCl_2$, MeOH, 25 °C, 30 min, 71%; c) BBr_3, dry DCM, from -78 to 25 °C, 12 h, 50%; d) TEA, dry THF, 25 °C, 12 h, 43-55%.

Structure–activity relationship studies and molecular modeling studies

The inhibition potency of compounds **5a–l** for the FAAH enzyme is reported in Table 1. Selectivity towards MAGL, CB_1R and CB_2R was evaluated for the most promising compounds. The new compounds showed an excellent selectivity profile for FAAH over MAGL, CB_1R, and CB_2R with only **5i** detecting a one digit micromolar affinity at CB_1R and a two digit micromolar affinity at CB_2R. The data confirmed that the presence of an "activated" electrophilic center (such as ureido or carbamoyl moieties) is a crucial prerequisite for potency. In fact compounds **5a-e**, where the electrophilic center is absent (**5d,e**) or where an urea is present between the two aliphatic amines (**5b-c**) were found inactive. When the urea involved an aniline (**5a**) as the carbamoylating moiety, enzyme inhibition was still poor although slightly higher than that of the other urea-containing analogues of the series. In line with our previous results, the insertion of a carbamate in the developed molecules allowed us to identify a series of selective FAAH inhibitors (**5f-l**) characterized by the presence of different scaffolds supporting the phenol moiety. The influence of polyethereal lateral chains (as the enzyme carbamoylating entities) was explored, for the most promising and synthetically accessible scaffolds, which modulated FAAH inhibition properties (**5j-l** *vs* **5i**).

Table 1. IC_{50} values on FAAH and MAGL enzymes, CB_1R and CB_2R for compounds **5a-l**, and reference compound **3**.

Cmpd	Structure	FAAH rat brain membrane IC_{50} nM (displacement %)[a,b]	MAGL COS cell cytosol (displacement %)[a,b]	CB_1R IC_{50} nM (displacement % at 50 µM)	CB_2R IC_{50} nM (displacement % at 50 µM)
5a	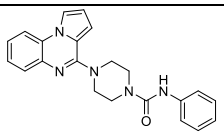	>50 µM (15.4)	NT[c]	NT[c]	NT[c]
5b	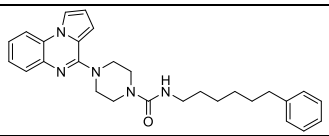	>50 µM (7.7)	NT[c]	NT[c]	NT[c]
5c	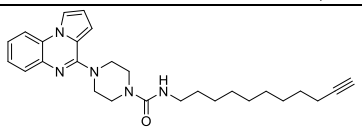	>50 µM (7.19)	NT[a]	NT[c]	NT[c]
5d	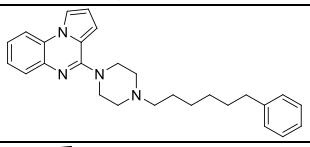	>50 µM (12.7)	NT[c]	NT[c]	NT[c]
5e	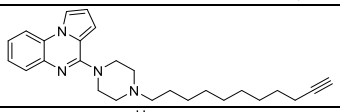	>50 µM (5.8)	NT[c]	NT[c]	NT[c]
5f	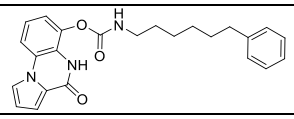	520	NT[c]	>50 µM (46.2)	>50 µM (6.6)
5g	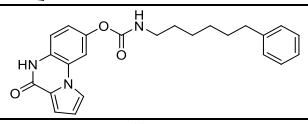	460	NT[c]	>50 µM (25.7)	>50 µM (4.3)
5h	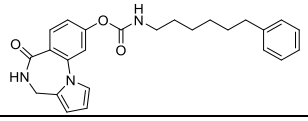	83.5	>50 µM (0.7)	>50 µM (25.3)	>50 µM (19.3)
5i	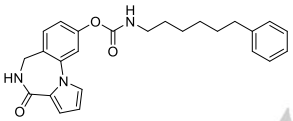	94.1	>50 µM (23.7)	6730	24300
5j	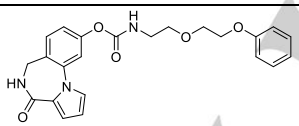	2825.3	>10 µM (5.7)	>50 µM (49.0)	>50 µM (25.5)
5k	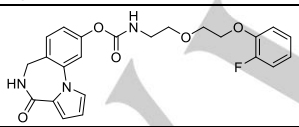	1672.3	>10 µM (7.5)	>50 µM (42.5)	>50 µM (39.3)
5l	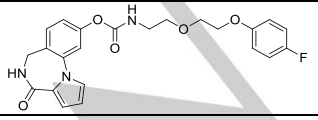	2687.3	>10 µM (6.8)	>50 µM (46.0)	>50 µM (37.4)
3[22]		0.60	NA[d]	NA[d]	NA[d]

[a]Values are means of three experiments (n = 3) and all SD not indicated are within 10%. [b]% of displacement at the maximum concentration tested is reported in brackets when IC_{50} is > 10 or 50 µM; tests were performed as previously described [25] with FAAH from rat brain (sequence identity of 82.7% and sequence similarity of 97.2% with *h*FAAH) or MAGL COS from cytosol with 30' or 20' of incubation time at 37 °C, respectively. [c]NT = Not tested. [d]NA = Not active.

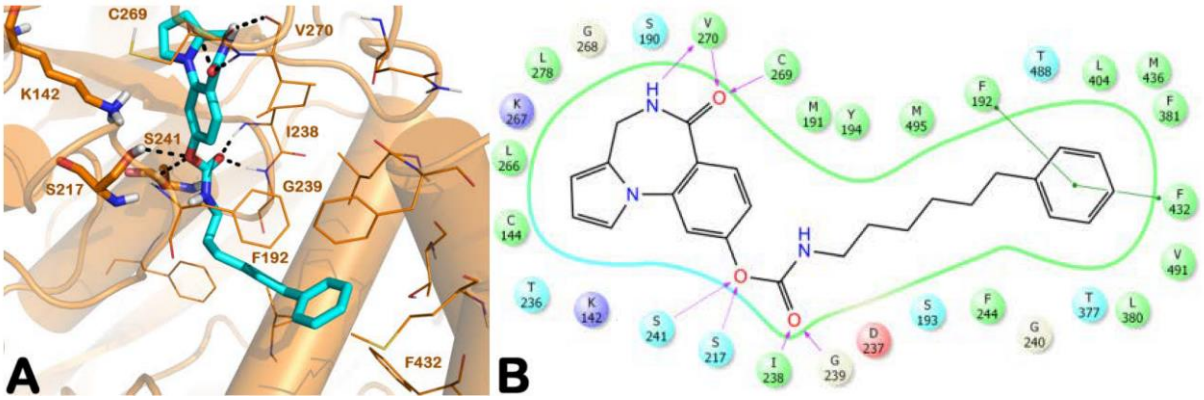

Figure 2. (A,B) IFD pose and ligand interaction diagram of compound **5h** (cyan sticks) into FAAH enzyme (PDB ID: 3PPM in orange cartoon). The catalytic triad of the enzyme is represented by sticks, while the key residues of the FAAH binding site are represented by lines. The H-bonds are represented by black dotted lines. Pictures generated by PyMOL and Maestro (Maestro, version 9.3, Schrödinger, LLC, New York, NY, 2012).

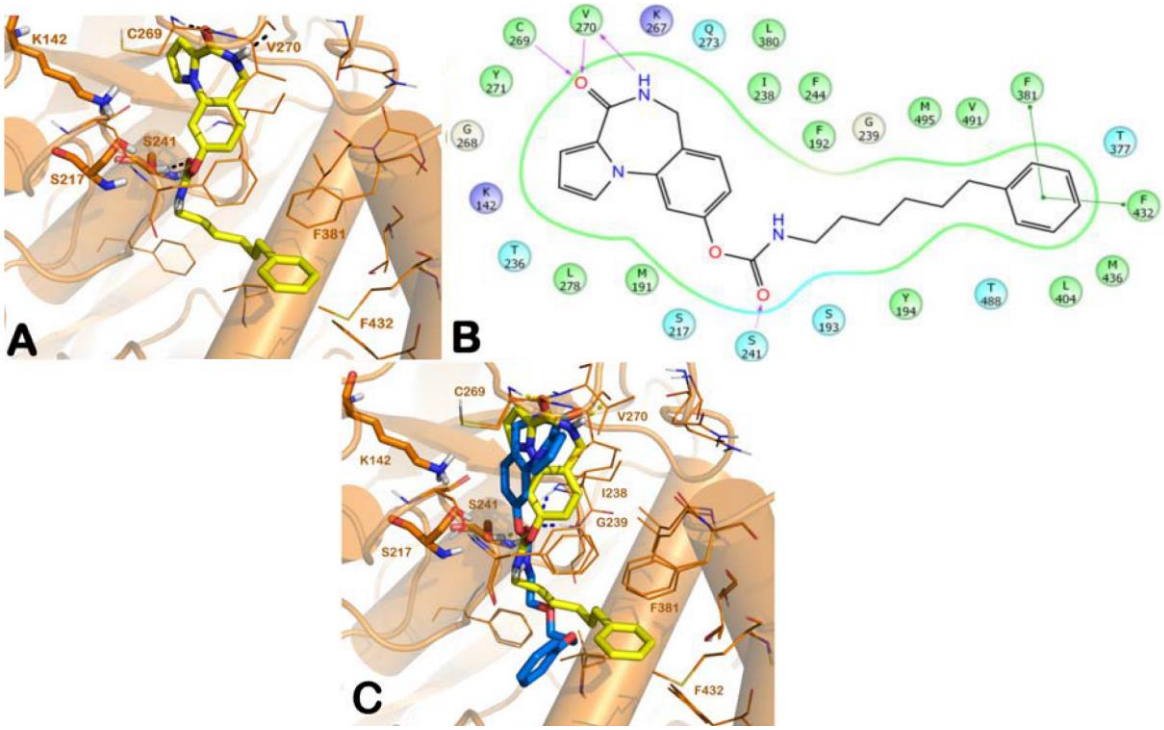

Figure 3. (A,B) IFD pose and ligand interaction diagram of compound **5i** (yellow sticks) into FAAH enzyme (PDB ID: 3PPM in orange cartoon). (C) Superposition between IFD poses of **5i** (yellow sticks) and **5j** (blue sticks). The catalytic triad of the enzyme is represented by sticks, while the key residues of the FAAH binding site are represented by lines. The H-bonds are represented by dotted lines. The pictures were generated by PyMOL and Pictures generated by PyMOL and Maestro (Maestro, version 9.3, Schrödinger, LLC, New York, NY, 2012).

To better understand the structure–activity relationships (SARs) of the developed compounds, we performed molecular docking studies to assess the interactions of the inhibitors with the FAAH enzyme at atomic level. We performed an Induced Fit Docking (IFD) calculation as reported,[33-35] to identify the main contacts governing the behavior of our compounds into the enzyme. The data were compared with those obtained by applying the same protocol to our previously described lead **3** (see Supplementary Information and Figure S1). In particular **5h**, one of the most potent compounds of this series, interacts with the FAAH active site by polar and hydrophobic contacts (Figure 2A, B). Polar contacts were established by the lactam moiety and the backbones of V270 and C269. In line with the potency of FAAH inhibition of **5h** (IC_{50} = 83.5 nM, Table 1) the electrophilic moiety is properly placed in front of the catalytic serine residues (S217 and S241) which can establish H-bonds with the carbamate phenate oxygen. The orientation of the carbon of the carbamate portion and its distance from the catalytic S241 (< 3Å) are in agreement with a potential nucleophilic attack. The carbonyl group can establish two H-bonds with the I238 and G239. Furthermore, the phenylhexyl lateral chain could be located in a sub-hydrophobic pocket, lined by F192, F381 and F432, producing a double π-π stacking with F192 and F432. Compound **5i** displayed similar interactions besides a correct orientation towards S241 (π-π stackings with F381 and F432, and H-bonds with C269 and V270, and, the interaction with the catalytic S241) (Figure 3A, B).

In compound **5j-l**, the introduction of a polyethereal tether, for replacing the hexyl chain of **5i** caused a marked decrease of FAAH inhibition. The docking outputs for **5j-l** clearly confirm the lack of potency (Figure S2A,B, S3A,B, S4A,B). The polyethereal chain is diverted from the accommodation in the hydrophobic sub-

pocket of the enzyme (see superposition of **5i** and **5j**, Figure 3C) and precludes the carbamate to establish interaction with S241the catalytic serine residue, while being still able to establish two H-bonds (with I238 and G239 for **5j** and with S193 and G239 for **5l** and **5k**).

In compound **5g** the restricted 6-6-5 tricyclic system produces a binding mode quite different from that found for the 6-7-5 system of **5h**. The tricyclic system can only form a H-bond with the backbone of C269, and in line with the three digit nanomolar potency of **5g** (Table 1) it lacks a suitable distance for interacting with S241. The different accommodation of the more planar and hindering tricyclic system prevents projecting the aliphatic tail into the hydrophobic sub-pocket (Figure S5A,B). The superposition of the IFD poses of **5h** and **5g** clearly traces out the described differences (Figure S5C).

The same is true for compound **5f** (Figure S6A, B). In particular, the tricyclic moiety establishes only one polar contact with T236. The carbamate group interacts with S217 and S241 by two H-bonds and the phenylhexyl tail forms a double π-π stacking with F192 and F381.

Cytotoxicity determination and antioxidant potential evaluation for 3, 5h, and 5i.

Oxidative stress (OS) plays a crucial role in neuropathic pain[36] and our working group provided evidence that it plays a crucial role in oxaliplatin-induced neuropathy.[37] On these bases, we decided to interrogate the ability of the most potent FAAH inhibitors of this series in the reduction of OS. Accordingly, the efficacy of compounds **5h** and **5i**, in comparison with our lead **3**, was measured in a cellular acute model of OS induced by hydrogen peroxide. By applying our previously described model,[38] a preliminary test was performed to assess the effects of the tested compounds in IMR32 cells morphology. As outlined in Figure S7 after treating the cells for 24 h with increasing concentrations of **3** and **5h,i** (with ranges between 0.1 to 50 μM), no changes were observed in cellular morphology.

We then tested the cytotoxicity profile in the same cell line by measuring the LDH release in the media, as measured by enzymatic assay (see Supplementary Material for details). As positive control (LDH amount corresponding to 100% cell death) IMR32 cells were treated with 1% Triton X-100, according to the manufacturer's instructions (Roche, Mannheim, Germany). Notably, no significant cytotoxic effect was observed for all the tested compounds at concentrations ranging from 0.1 μM to 50 μM (Figure S8).

These results with **3**, **5h** and **5i** prompted us to evaluate their potential anti-inflammatory and neuroprotective properties after treating the cells with pro-inflammatory substances. In order to find the most appropriate model for probing anti-inflammatory potential of our molecules in the IMR32 cell line we tested several pro-inflammatory mediators. Therefore, we first evaluated the activation of NF-kB by measuring the translocation to the nucleus of its cytoplasmic subunit p65. Accordingly, we treated the cells with lipopolysaccharide (LPS 100 μg/mL and 200 μg/mL) for 30, 60 and 90 min. The 100 μg treatment after 30 min was the most effective, in which we could clearly observe the nuclear translocation of p65 protein (see in Figure S9 the increment of the LPS bar with respect to the control bar). Thus, according to our protocol, we pre-treated the cells with compounds **3**, **5h** and **5i** for 24 h and subsequently with 100 μg/mL of LPS for 30 min. As shown in Figure S9 the pre-treatment was able to decrease p65 translocation with respect to the only LPS treated cells. Notably, while **5i** explicated its higher anti-inflammatory action at 1 μM concentration, compound **5h** exerted an anti-inflammatory effect inversely proportional to the dose.

***In vivo* efficacy: effect of acute administration of compounds 3, 5h and 5i on oxaliplatin induced neuropathic pain.**

We evaluated the effect of compounds **3**, **5h** and **5i** in a mouse model of neuropathic pain: the chemotherapy-dependent neuropathy induced by oxaliplatin.[39-40]

The repeated administration of the neurotoxic anticancer agent (2.4 mg kg^{-1}, i.p.) evoked an allodynia-like behavior measurable as increased sensitivity to a non-noxious cold stimulus (Cold plate test). On day 14, the licking latency decreased to 10.7 ± 0.9 s in comparison ($P<0.01$) to control mice (20.1 ± 0.8 s) treated with vehicle (Figure 4). FAAH inhibitors were tested in oxaliplatin-treated animals on day 14 and the pain relieving effects were evaluated over time after a single orally administered dose of the tested compounds. We initially established that our potent and selective FAAH inhibitor **3** was able to dose dependently increase the pain threshold already at 3 and 10 mg kg^{-1} peaking 30 min after treatment. On these bases, we decided to test the analogues **5h** and **5i** (in a dose range of 3 - 30 mg kg^{-1} p.o.). As shown in Figure 4, both compounds induced a significant relief of oxaliplatin-induced neuropathic pain starting from 3 mg kg^{-1}. Higher effects were obtained using **5h** and **5i**, administered at doses of 10 and 30 mg kg^{-1}. These dosages were equally effective between 15 and 30 min after administration. **5h** was significantly effective up to 45 min (Figure 4).

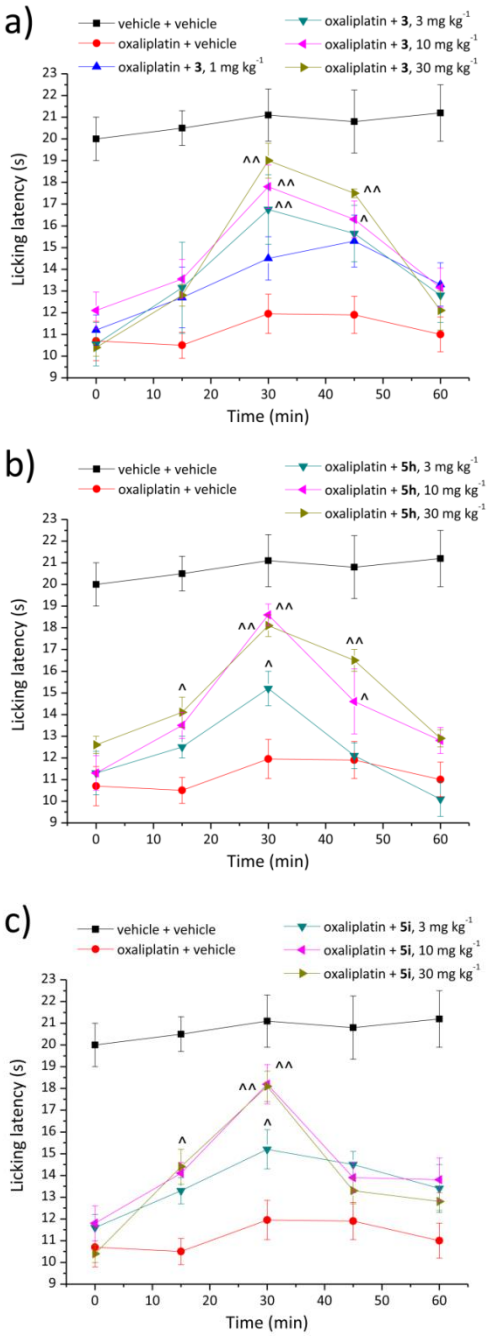

Figure 4. Pain relieving effect of compounds **3**, **5h** and **5i.** Mice were treated with oxaliplatin (2.4 mg kg^{-1} i.p., daily for 5 consecutive days every week for 2 weeks) to induce a painful neuropathy. Tested compounds were administered p.o. on day 14, control animals were treated with vehicles. Pain threshold was evaluated measuring the licking latency to a cold non-noxious stimulus (Cold plate test). Each value represents the mean ± S.E.M. of 12 mice performed in 2 different experimental sets. ^P<0.05 and ^^P<0.01 in respect to the value before treatment.

Conclusions

The FAAH enzyme significantly contributes in terminating EC signaling and represents a relevant therapeutic target. By inhibition of the ECs metabolizing enzymes, we can attain indirect agonism at CBRs, and therapeutic efficacy devoid of psychotropic effects. Aiming at discovering new selective FAAH inhibitors, in this manuscript we have described the development and SAR analysis of a series of new analogues (**5a-l**) bearing functionalized tricyclic scaffolds and structurally inspired to our previous ligands **3** and **4**. The developed compounds showed an excellent selectivity profile for FAAH over MAGL, CB_1R, and CB_2R with **5i** detecting some (micromolar) affinity at CBRs. The most potent FAAH inhibitors of the series **5h** and **5i** were used for further studies. When studied on a neuroblastoma cell line (IMR32) **5h**, **5i** and our reference compound **3** demonstrated the absence of cytotoxic effects and the ability to reduce OS by decreasing the expression of the redox-sensitive transcription factor NF-kB. The efficacy of the same compounds was also assessed *in vivo* in a rodent model of neuropathic pain. After oral administration at 10 mg/kg all the compounds (**5h**, **5i** and **3**) were able to relieve the hypersensitivity induced by oxaliplatin.

Experimental Section

Chemistry

Unless otherwise specified, materials were purchased from commercial suppliers and used without further purification. Reaction progress was monitored by TLC using silica gel 60 F254 (0.040–0.063 mm) with detection by UV. Silica gel 60 (0.040–0.063 mm) was used for column chromatography. 1H NMR and 13C NMR spectra were recorded on a Varian 300 MHz spectrometer or a Bruker 400 MHz spectrometer by using the residual signal of the deuterated solvent as internal standard. Splitting patterns are described as singlet (s), doublet (d), triplet (t), quartet (q) and broad (br); the values of chemical shifts (δ) are given in ppm and coupling constants (J) in Hertz (Hz). Microwave reactions were performed by a CEM Discovery apparatus. ESI/MS spectra were performed by an Agilent 1100 Series LC/MSD spectrometer. HRESIMS were carried out by a Thermo Finningan LCQ Deca XP Max ion-trap mass spectrometer equipped with Xcalibur software, operated in positive ion mode. The yields are referred to purified products and are not optimized. All moisture-sensitive reactions were performed under argon atmosphere using oven-dried glassware and anhydrous solvents. Final compounds were analyzed by combustion analysis (CHN) to confirm purity >95%.

***N*-Phenyl-4-(pyrrolo[1,2-*a*]quinoxalin-4-yl)piperazine-1-carboxamide (5a).** Compound **6** (60 mg, 0.24 mmol) was dissolved in dry THF (2.0 mL) and TEA (33 µL, 0.24 mmol) was added. Then phenyl isocyanate (**7a**) (52 µL, 0.47 mmol) was added dropwise and the reaction mixture was heated under reflux for 12 h. After reaction completion volatiles were removed in vacuo and the residue was purified. Column chromatography on silica gel (*n*-hexane/EtOAc 2:1) provided pure title compound (62% yield) as a pale yellow solid. ^{1}H NMR (300 MHz, $CDCl_3$) δ 3.74 (m, 4H), 3.91 (m, 4H), 6.45 (br s, 1H), 6.79 (m, 2H), 7.06 (m, 2H), 7.26-7.41 (m, 5H), 7.67-7.76 (m, 2H), 7.85 (m, 1H). ^{13}C-NMR (75 MHz, $CDCl_3$) δ 43.7, 47.5, 106.7, 112.6, 113.3, 114.6, 120.0 (2C), 123.3 (2C), 124.3, 125.2, 125.8, 127.5, 128.9 (2C), 152.3, 155.0. ESI-MS *m/z* 372 $[M + H]^+$ (100), 394 $[M + Na]^+$. Elemental analysis calcd (%) for $C_{22}H_{21}N_5O$: C 71.14, H 5.70, N 18.85; found: C 71.08, H 5.93, N1 8.70.

***N*-(6-Phenylhexyl)-4-(pyrrolo[1,2-*a*]quinoxalin-4-yl)piperazine-1-carboxamide (5b).** The title compound was prepared according to the procedure previously described for **5a** starting from **6** (100 mg, 0.40 mmol), TEA (56 µL, 0.40 mmol) and 6-phenyl-1-hexylisocyanate (**7b**) (161 mg, 0.79 mmol). Column chromatography on silica gel (*n*-hexane/EtOAc 1:1) provided pure title compound (59% yield) as a pale yellow amorphous solid. ^{1}H NMR (300 MHz, $CDCl_3$) δ 1.28-1.67 (m, 8H), 2.62 (t, *J* = 7.8 Hz, 2H), 3.26 (m, 2H), 3.59 (m, 4H), 3.84 (m, 4H), 4.64 (br t, 1H), 6.77 (m, 2H), 7.15-7.36 (m, 7H), 7.68 (m, 2H), 7.82 (m, 1H). ESI-MS *m/z* 456 $[M + H]^+$,(100) 478 $[M + Na]^+$. Elemental analysis calcd (%) for $C_{28}H_{33}N_5O$: C 73.82, H 7.30, N 15.37; found: C 73.75, H 7.51, N 15.71.

***N*-(Undec-10-yn-1-yl)-4-(pyrrolo[1,2-*a*]quinoxalin-4-yl)piperazine-1-carboxamide (5c).** The title compound was prepared according to the procedure described for **5a** starting from **6** (72 mg 0.29 mmol), TEA (40 µL, 0.29 mmol) and undec-10-yn-1-yl isocyanate (**7c**) (110 mg, 0.57 mmol). Column chromatography on silica gel (*n*-hexane/EtOAc 2:1) provided pure title compound (60% yield) as a pale yellow amorphous solid. ^{1}H NMR (300 MHz, $CDCl_3$) δ 1.23-1.54 (m, 14H), 1.94 (m, 1H), 2.18 (m, 2H), 3.26 (m, 2H), 3.60 (m, 4H), 3.84 (m, 4H), 4.53 (br t, 1H), 6.78 (m, 2H), 7.26-7.32 (m, 2H), 7.64-7.74 (m, 2H), 7.83 (s, 1H). ESI-MS *m/z* 446 $[M + H]^+$, (100) 468 $[M + Na]^+$. Elemental analysis calcd (%) for $C_{27}H_{35}N_5O$: C 72.78, H 7.92, N 15.72; found: C 72.73 , H 8.14, N 16.03.

4-(4-(6-Phenylhexyl)piperazin-1-yl)pyrrolo[1,2-*a*]quinoxaline (5d). 6-Phenylhexylbromide (96 mg, 0.40 mmol) was dissolved in MeCN (HPLC grade, 4.0 mL) and the solution was heated to reflux. Then, compound **6** (100 mg, 0.40 mmol) was added, followed by TEA (61 µL, 0.44 mmol). The reaction mixture was heated under reflux for 12 h and the volatiles were evaporated in vacuo. Column chromatography on silica gel (*n*-hexane/EtOAc 2:1) provided pure title compound (75% yield) as a pale yellow oil. ^{1}H NMR (300 MHz, $CDCl_3$) δ 1.39-1.69 (m, 8H), 2.42 (m, 2H), 2.64 (m, 6H), 3.85 (m, 4H), 6.78 (m, 2H), 7.19-7.30 (m, 7H), 7.72 (m, 2H), 7.81 (m, 1H). ^{13}C-NMR (75 MHz, $CDCl_3$) δ 22.8, 23.5, 25.3, 25.3, 27.5, 32.0, 44.0 (2), 49.4 (2), 54.9, 102.8, 108.4, 109.3, 110.4, 116.3, 119.9, 121.2, 121.6, 121.8, 123.5, 124.3 (2C), 124.4 (2C), 132.3, 138.8, 148.6. ESI-MS *m/z* 413 $[M + H]^+$. Elemental analysis calcd (%) for $C_{27}H_{32}N_4$: C 78.60, H 7.82, N 13.58; found: C 78.87, H 7.68, N 13.35.

4-(4-(Undec-10-yn-1-yl)piperazin-1-yl)pyrrolo[1,2-*a*]quinoxaline (5e). The title compound was prepared according to the procedure described for **5d** starting from **6** (55 mg, 0.22 mmol), undec-10-yn-1-yl bromide (50 mg, 0.22 mmol) and TEA (33 µL, 0.24 mmol). Column chromatography on silica gel (*n*-hexane/EtOAc 2:1) provided pure title compound (71% yield) as a pale yellow oil. ^{1}H NMR (300 MHz, $CDCl_3$) δ 1.26-1.56 (m, 14H), 1.94 (m, 1H), 2.20 (m, 2H), 2.41 (m, 2H), 2.64 (m, 4H), 3.84 (m, 4H), 6.76 (m, 2H), 7.22-7.35 (m, 2H), 7.67 (m, 2H), 7.81 (m, 1H). ESI-MS *m/z* 403 $[M + H]^+$. Elemental analysis calcd (%) for $C_{26}H_{34}N_4$: C 77.57, H 8.51, N 13.92; found C 77.73, H 8.38, N 14.09.

***tert*-Butyl 3-methoxy-2-nitrophenylcarbamate (9).** To a solution of 3-methoxy-2-nitrobenzoic acid (**8**) (1 g, 5.08 mmol) in 20.0 mL of *tert*-butanol were added diphenylphosphoryl azide (1.15 mL, 5.36 mmol) and TEA (0.75 mL, 5.42 mmol). The reaction mixture was heated to reflux for 15 h, then cooled to 25 °C and solvents were removed by rotary evaporation. Residue was taken up with EtOAc and washed with a saturated aqueous solution of NH_4Cl, water, a saturated solution of $NaHCO_3$ and brine. The organic layer was dried over anhydrous Na_2SO_4, filtered and concentrated affording the title compound (78% yield). ^{1}H NMR (300 MHz, $CDCl_3$) δ 1.38 (s, 9H), 3.83 (s, 3H), 6.68 (dd, *J* = 7.5, 1.5 Hz, 1H), 7.71 (t, *J* = 7.5 Hz, 1H), 8.09 (dd, *J* = 7.5, 1.5 Hz, 1H), 9.15 (br s, 1H). ESI-MS *m/z* 291 $[M + Na]^+$ (100).

3-Methoxy-2-nitroaniline (10). Compound **9** (1.2 g, 4.47 mmol) was dissolved in 1.4 mL of TFA and the resulting solution was stirred at 0 °C for 1.5 h. Then the solvent was evaporated and the residue was dissolved in EtOAc and washed with a saturated aqueous $NaHCO_3$. The organic phase was dried over anhydrous Na_2SO_4, filtered and concentrated affording the title compound (99% yield). ^{1}H NMR (300 MHz, $CDCl_3$) δ 3.87 (s, 3H), 4.43 (brs, 2H), 6.30 (dd, *J* = 8.2, 0.9 Hz, 1H), 6.36 (dd, *J* = 7.5, 1.5 Hz, 1H), 7.16 (t, *J* = 8.2 Hz, 1H). ESI-MS *m/z* 169 $[M + H]^+$.

1-(3-Methoxy-2-nitrophenyl)-1*H*-pyrrole (11). To a solution of 3-methoxy-2-nitroaniline **10** (500 mg, 2.97 mmol) in acetic acid (10.0 mL) and water (2.0 mL), 2,5-dimethoxytetrahydrofuran (385 µL, 2.97 mmol) in acetic acid (1.0 mL) was added dropwise. The solution was heated at 100 °C for 15 min. After removal of the solvent, the dark-brown reaction mixture was diluted with EtOAc and neutralized with an aqueous saturated solution of Na_2CO_3. Then, it was extracted with EtOAc (3 × 100 mL), dried over anhydrous Na_2SO_4, filtered, and concentrated. Compound **11** (97% yield) was obtained as a colourless solid. ^{1}H NMR (300 MHz, $CDCl_3$) δ 3.83 (s, 3H), 6.41 (d, *J* = 1.5 Hz, 2H), 6.94 (dd, *J* = 7.5, 1.5 Hz, 1H), 7.26 (d, *J* = 1.5 Hz, 2H), 7.44 (dd, *J* = 7.5, 1.5 Hz, 1H), 7.73 (t, *J* = 8.2 Hz, 1H). ESI-MS *m/z* 219 $[M + H]^+$.

2-Methoxy-6-(1*H*-pyrrol-1-yl)aniline (12). To a solution of 1-(3-methoxy-2-nitrophenyl)-1*H*-pyrrole (**11**) (680 mg, 3.12 mmol) in 75% ethanol (8.0 mL), calcium chloride (229 mg, 1.56 mmol) and iron powder (1.23 g, 7.09 mmol) were added. The reaction mixture was heated under reflux for 2 h, then was filtered through a celite pad. The solvent was removed and the residue was dissolved in chloroform and washed with water. The organic phase was dried over anhydrous Na_2SO_4, filtered and concentrated. The compound was submitted to the subsequent step without further purification (87% yield). ^{1}H NMR (300 MHz, $CDCl_3$) δ 3.83 (s, 3H), 6.27 (brs, 2H), 6.41 (d, *J* = 1.5 Hz, 2H), 6.70 (t, *J* = 8.2 Hz, 1H), 6.85 (dd, *J* = 7.5, 1.5 Hz, 1H), 6.93 (dd, *J* = 7.5, 1.5 Hz, 1H), 7.26 (d, *J* = 1.5 Hz, 2H). ESI-MS *m/z* 189 $[M + H]^+$.

6-Methoxypyrrolo[1,2-*a*]quinoxalin-4(5*H*)-one (13). To a solution of **12** (1.83 g, 9.73 mmol) in toluene (26.0 mL), triphosgene (778 mg, 2.63 mmol) was added and the resulting solution was heated under reflux for 2 h. Then the reaction mixture was cooled under nitrogen flow and the solvent was evaporated. The residue was purified by silica gel column chromatography (chloroform/EtOAc 2:1) affording the title compound (52% yield) as colourless solid. ^{1}H NMR (300 MHz, $CDCl_3$) δ 3.97 (s, 3H), 6.67-6.69 (m, 1H), 6.81 (dd, *J* = 8.2, 0.9 Hz, 1H), 7.14 (t, *J* = 8.2 Hz, 1H), 7.25-7.28 (m, 2H), 7.64-7.65 (m, 1H), 8.42 (br s, 1H). ESI-MS *m/z* 215 $[M + H]^+$.

6-Hydroxypyrrolo[1,2-a]quinoxalin-4(5*H*)-one (14). To a suspension of 6-methoxypyrrolo[1,2-*a*]quinoxalin-4(5*H*)-one (**13**) (100 mg, 0.47 mmol) in dry DCM (6.0 mL), boron tribromide (1M solution in DCM, 1.87 mL, 1.87 mmol) was added at −78 °C. The reaction mixture was then allowed to warm to room temperature and stirred for 12 h. A saturated aqueous solution of Na_2CO_3 was added to quench the reaction. The residue was extracted with EtOAc (3 × 20 mL). The combined organic extracts were dried over anhydrous Na_2SO_4, filtered, and concentrated. Column chromatography (chloroform/EtOAc 1:1) provided the title compound (11% yield) as a colourless solid. ^{1}H NMR (300 MHz, CD_3OD) δ 6.68-6.70 (m, 1H), 6.79 (d, *J* = 8.2 Hz, 1H), 7.07 (t, *J* = 8.2 Hz, 1H), 7.18 (d, *J* = 2.9 Hz, 1H), 7.34 (d, *J* = 8.2 Hz, 1H), 7.92 (s, 1H). ESI-MS *m/z* 199 $[M-H]^-$.

4-Oxo-4,5-dihydropyrrolo[1,2-*a*]quinoxalin-6-yl 6-phenylhexylcarbamate (5f). The title compound was prepared according to the procedure described for **5a** starting from 6-hydroxypyrrolo[1,2-*a*]quinoxalin-4(5*H*)-one **14** (10 mg, 0.05 mmol), phenylhexyl isocyanate **7b** (41 mg, 0.20 mmol) and TEA (28 µL, 0.20 mmol). Column chromatography (chloroform) afforded the title compound (30% yield) as a colourless solid. ^{1}H NMR (300 MHz, $CDCl_3$) δ 1.36 (m, 4H), 1.57 (m, 4H), 2.55 (t, *J* = 7.5 Hz, 2H), 3.31 (t, *J* = 5.9 Hz, 2H), 6.70 (d, *J* = 2.3 Hz, 1H), 7.11-7.26 (m, 7H), 7.46 (d, *J* = 8.5 Hz, 1H), 7.61 (d, *J* = 8.2 Hz, 1H), 7.70 (s, 1H), 10.95 (s, 1H). ^{13}C-NMR (75 MHz, $CDCl_3$) δ 26.9, 29.1, 30.1, 31.5, 36.1, 41.6, 110.3, 112.4, 113.7, 117.8, 118.7, 120.8, 123.0, 124.2, 125.5, 125.8, 128.5 (2), 128.6 (2), 139.7, 142.9, 153.6, 156.7. ESI-MS *m/z* 426 $[M + Na]^+$. Elemental analysis calcd (%) for $C_{24}H_{25}N_3O_3$: C 71.44, H 6.25, N 10.41; found: C 71.76, H 6.09, N 10.27.

***N*-(5-Hydroxy-2-nitrophenyl)acetamide (16).** To a solution of **15** (1.0 g, 6.62 mmol) in acetic anhydride (5.0 mL), a mixture of conc. HNO_3 (3.6 mL) and acetic acid (3.6 mL) was added and the reaction was stirred at 25 °C for 8 h. 2N HCl (5.0 mL) was added to quench the excess of acetic anhydride and the mixture was diluted with water. The resulting precipitate was filtered and washed with cold water to afford the pure title compound (98% yield) as a yellow solid. ^{1}H NMR

(300 MHz, $CDCl_3$) δ 2.24 (s, 3H), 7.07 (d, *J* = 7.6 Hz, 1H), 7.35 (br s, 1H), 7.46 (s, 1H), 8.07 (d, *J* = 9.4 Hz, 1H), 10.82 (s, 1H). ESI-MS *m/z* 195 $[M-H]^-$.

4-Amino-3-(1*H*-pyrrol-1-yl)phenol (17). Compound **16** (1.2 g, 6.49 mmol) was dissolved in concentrated HCl (10.0 mL) and the resulting suspension was stirred at 110 °C for 5 min. The mixture was cooled to 25 °C, diluted with water and the aqueous phase was extracted with EtOAc (3 x 15.0 mL). The combined organic layers were dried over Na_2SO_4, filtered, and concentrated to afford the intermediate *3-amino-4-nitrophenol* (95% yield) that was carried on without any further purification. ^{1}H NMR (300 MHz, acetone-*d*6) δ 6.24 (dd, *J* = 9.4, 2.6 Hz, 1H), 6.45 (d, *J* = 2.4 Hz, 1H), 7.01 (br s, 2H), 7.97 (d, *J* = 9.4 Hz, 1H), 9.37 (s, 1H). ESI-MS *m/z* 153 $[M-H]^-$. A stirred solution of *3-amino-4-nitrophenol* (950 mg, 6.17 mmol) and 2,5-dimethoxytetrahydrofuran (960 µL, 7.41 mmol) in 1,4-dioxane (20.0 mL), was stirred at 120 °C for 15 min before adding 5N HCl (1.5 mL). The mixture was stirred at 110 °C for further 5 min, then cold water was added and the resulting white precipitate was filtered and washed with cold water to afford the pure *4-nitro-3-(1H-pyrrol-1-yl)phenol* (70% yield) as an amorphous solid. ^{1}H NMR (300 MHz, $CDCl_3$) δ 6.36 (d, *J* = 1.5 Hz, 2H), 6.79 (d, *J* = 1.5 Hz, 2H), 6.85 (s, 1H), 7.17 (d, *J* = 2.6 Hz, 1H), 7.92 (d, *J* = 8.5 Hz). ESI-MS *m/z* 203 $[M-H]^-$.

To a solution of *4-nitro-3-(1H-pyrrol-1-yl)phenol* (400 mg, 1.96 mmol) in EtOAc (10.0 mL) $SnCl_2{\cdot}2H_2O$ (2.2 g, 9.8 mmol) was added and the reaction was stirred at 25 °C for 2 h. A saturated solution of $NaHCO_3$ was added and the aqueous phase was extracted with EtOAc (3 x 20.0 mL). The combined organic layers were dried over Na_2SO_4, filtered and evaporated. The crude was purified by means of chromatography on silica gel (petroleum ether/diethyl ether 3:2) to give pure compound **17** (85% yield) as a colourless solid. ^{1}H NMR (300 MHz, $CDCl_3$) δ 4.09 (br s, 2H), 6.33 (s, 2H), 6.62-6.67 (m, 3H), 7.80 (s, 2H), 7.16 (s, 1H). ESI-MS *m/z* 175 $[M + H]^+$.

8-Hydroxypyrrolo[1,2-*a*]quinoxalin-4(5*H*)-one (18). Starting from **17** (100 mg, 0.57 mmol), the title compound was obtained following the same procedure reported for **13**. The crude was purified by means of chromatography on silica gel (MeOH/chloroform 1:20) to provide title compound (36% yield) as a colourless solid. ^{1}H NMR (300 MHz, DMSO-*d*6) δ 6.63 (m, 1H), 6.73-6.76 (m, 1H), 6.70 (m, 1H), 7.09-7.12 (m, 1H), 7.36 (s, 1H), 8.01 (m 1H), 9.57 (s, 1H), 11.00 (s, 1H). ESI-MS *m/z* 199 $[M-H]^-$.

4-Oxo-4,5-dihydropyrrolo[1,2-*a*]quinoxalin-8-yl 6-phenylhexylcarbamate (5g). Starting from **18** (40 mg, 0.20 mmol) and 6-phenylhexyl isocyanate (165 mg, 0.80 mmol), the title compound was obtained following the same procedure reported for **5a**. The crude was purified by means of chromatography on silica gel (diethyl ether/chloroform 2:1) to afford title compound (10% yield) as a colourless solid. ^{1}H NMR (300 MHz, CD_3OD) δ 1.39-1.42 (m, 4H), 1.55-1.67 (m, 4H), 2.58 (t, *J* = 7.5 Hz, 2H), 3.18 (t, *J* = 7.0 Hz, 2H), 6.69-6.71 (m, 1H), 7.05 (dd, *J* = 8.8, 2.4 Hz, 1H), 7.13-7.30 (m, 7H), 7.73 (d, *J* = 2.4 Hz, 1H), 7.94-7.96 (m, 1H); ^{13}C-NMR (75 MHz, CD_3OD) δ 26.5, 28.8, 29.5, 31.5, 35.7, 40.9, 108.6, 112.3, 113.2, 117.2, 118.2, 119.4, 123.0, 123.7, 125.5 (2C), 128.1 (2C), 128.2 (2C), 142.7, 147.3, 155.9, 156.7. ESI-MS *m/z* 426 $[M + Na]^+$. Elemental analysis calcd (%) for $C_{24}H_{25}N_3O_3$: C 71.44, H 6.25, N 10.41; found: C 71.37, H 6.51, N 10.58.

Methyl 4-methoxy-2-(1*H*-pyrrol-1-yl)benzoate (20). To an ice-cooled solution of **19** (1.0 g, 5.07 mmol) in MeOH (10.0 mL), $SOCl_2$ (740 µL, 10.15 mmol) was added dropwise and the reaction mixture was stirred at 25 °C for 10 h. Solvent was removed under reduced pressure and the residue was taken up with EtOAc and washed with a saturated solution of $NaHCO_3$. The organic phase was dried over Na_2SO_4, filtered and evaporated to obtain *methyl 4-methoxy-2-nitrobenzoate* (quantitative yield) which was carried on without any further purification. ^{1}H NMR (300 MHz, $CDCl_3$) δ 3.84 (s, 3H), 3.99 (s, 3H), 7.31 (dd, *J* = 8.8, 2.6 Hz, 1H), 7.42 (d, *J* = 2.6 Hz, 1H), 7.88 (d, *J* = 8.8 Hz, 1H). ESI-MS *m/z* 212 $[M + H]^+$ .To a solution of *methyl 4-methoxy-2-nitrobenzoate* (5.07 mmol) in EtOAc (10.0 mL) $SnCl_2{\cdot}2H_2O$ (3.57 g, 15.84 mmol) was added and the reaction was stirred at 25 °C for 2 h. The reaction was quenched with a saturated solution of $NaHCO_3$ and the aqueous phase was extracted with EtOAc (3 x 25.0 mL). The combined organic layers were dried over Na_2SO_4, filtered and evaporated to afford *methyl 2-amino-4-methoxybenzoate* (quantitative yield) as a pale yellow solid which was used in the next step without any further purification. ^{1}H NMR (300 MHz, $CDCl_3$) δ 3.78 (s, 3H), 3.83 (s, 3H), 5.52 (br s, 2H), 6.11 (d, *J* = 2.4 Hz, 1H), 6.23 (dd, *J* = 9.1, 2.4 Hz, 1H), 7.78 (d, *J* = 9.1, 1H). ESI-MS *m/z* 182 $[M + H]^+$, 204 $[M + Na]^+$.

Starting from *methyl 2-amino-4-methoxybenzoate* (300 mg, 1.70 mmol), the title compound was obtained following the same procedure reported for **17**. The crude was purified by means of chromatography on silica gel (petroleum ether/chloroform 1:1) to afford pure compound **20** (87% yield) as a withe solid. ^{1}H NMR (300 MHz, $CDCl_3$) δ 3.70 (s, 3H), 3.83 (s, 3H), 6.32 (t, *J* = 2.2 Hz, 2H), 6.82 (t, *J* = 2.2 Hz, 2H), 6.87-6.91 (m, 2H), 7.84 (d, *J* = 8.3 Hz, 1H). ESI-MS *m/z* 254 $[M + Na]^+$.

Methyl 2-(2-cyano-1*H*-pyrrol-1-yl)-4-methoxybenzoate (21). To an ice-cooled solution of dry DMF (1.0 mL) and dry 1,2-DCE (2.0 mL), $(COCl)_2$ (135 µL, 1.55 mmol) was added. The mixture was allowed to warm to 25 °C and stirred for 15 min. Then it was cooled to 0 °C and a solution of **20** (325 mg, 1.41 mmol) in dry 1,2-DCE (1.0 mL) was added. The reaction was stirred at 25 °C for further 15 min. A solution of $NH_2OH{\cdot}HCl$ (108 mg, 1.55 mmol) and pyridine (125 µL, 1.55 mmol) in dry DMF (1.0 mL) was added and the mixture was stirred at 120 °C for 10 h. A saturated solution of $NaHCO_3$ was added dropwise and the aqueous phase was extracted with EtOAc (3 x 10.0 mL). The combined organic layers were dried over anhydrous Na_2SO_4, filtered, and evaporated. The crude was purified by means of chromatography on silica gel (petroleum ether/diethyl ether 1:1) to afford title compound (47% yield) as a colourless solid. ^{1}H NMR (300 MHz, $CDCl_3$) δ 3.72 (s, 3H), 3.90 (s, 3H), 6.33-6.35 (m, 1H), 6.89 (d, *J* = 2.6 Hz, 1H), 6.92-6.94 (m, 1H), 6.97 (dd, *J* = 4.0, 1.6 Hz, 1H), 7.03 (dd, *J* = 8.8, 2.3 Hz, 1H), 8.06 (d, *J* = 8.8 Hz, 1H). ESI-MS *m/z* 279 $[M + Na]^+$.

9-Methoxy-4*H*-benzo[*f*]pyrrolo[1,2-*a*][1,4]diazepin-6(5*H*)-one (22). To a stirred suspension of **21** (290 mg, 1.13 mmol) and $CoCl_2$ (294 mg, 2.26 mmol) in MeOH (10.0 mL), $NaBH_4$ (420 mg, 11.30 mmol) was added and reaction was stirred at 25 °C for 20 min. 2 N HCl was added and solvent was removed under reduced pressure. The solution was basified with 2 N NaOH and the aqueous phase was extracted with ethyl acetate (3 x 10.0 mL). The combined organic layers were dried over Na_2SO_4, filtered, and evaporated. The crude was purified by means of chromatography on silica gel (EtOAc) to afford title compound (64% yield) as a colourless solid. ^{1}H NMR (300 MHz, $CDCl_3$) δ 3.90 (s, 3H), 4.20 (br d, 2H), 6.12 (s, 1H), 6.28 (s, 1H), 6.87-6.92 (m, 2H), 7.03 (s, 1H), 7.32 (br s, 1H), 7.97 (d, *J* = 8.8 Hz, 1H). ESI-MS *m/z* 229 $[M + H]^+$, 251 $[M + Na]^+$.

6-Oxo-5,6-dihydro-4*H*-benzo[*f*]pyrrolo[1,2-*a*][1,4]diazepin-9-yl-6-phenylhexylcarbamate (5h). Starting from **22**, *hydroxy-4H-benzo[f]pyrrolo[1,2-a][1,4]diazepin-6(5H)-one* was obtained following the same procedure reported for **14**. The crude was purified by means of chromatography on silica gel (chloroform/EtOAc 1:1) to afford compound *hydroxy-4H-benzo[f]pyrrolo[1,2-a][1,4]diazepin-6(5H)-one* (50% yield) as a colourless solid. ^{1}H NMR (300 MHz, acetone-*d*6) δ 4.22 (s, 2H), 6.11 (d, *J* = 2.3 Hz, 1H), 6.20-6.24 (m, 1H), 6.85-6.93 (m, 2H), 7.10-7.12 (m, 1H), 7.81-7.86 (m, 2H), 9.42 (br s, 1H). ESI-MS *m/z* 213 $[M-H]^-$. Starting from *hydroxy-4H-benzo[f]pyrrolo[1,2-a][1,4]diazepin-6(5H)-one* (14 mg, 0.06 mmol) and 6-phenylhexyl isocyanate **7b** (50 mg, 0.25 mmol), the title compound was obtained following the same procedure reported for **5a**. The crude was purified by means of chromatography on silica gel (MeOH/DCM 1:20) to afford title compound **5h** (60% yield) as a colourless solid. ^{1}H NMR (300 MHz, $CDCl_3$) δ 1.38-1.41 (m, 4H), 1.57-1.70 (m, 4H), 2.62 (t, *J* = 7.6

Hz, 2H), 3.27 (q, *J* = 6.1 Hz, 2H), 4.21 (s, 2H), 5.14 (br s, 1H), 6.11 (br d, 1H), 6.27 (t, *J* = 2.9 Hz, 1H), 7.01 (br d, 1H), 7.12-7.31 (m, 7H), 7.96 (d, *J* = 8.5 Hz, 1H); ^{13}C NMR (75 MHz, $CDCl_3$) δ 26.8, 29.1, 29.9, 31.6, 36.1, 37.7, 41.6, 107.3, 110.8, 115.7, 119.3, 120.9, 125.9, 128.5 (2C), 128.6 (2C), 132.2, 133.6, 138.6, 142.8, 153.7, 154.6, 169.6. ESI-MS *m/z* 418 $[M + H]^+$.

Elemental analysis calcd (%) for $C_{25}H_{27}N_3O_3$: C 71,92, H 6,52, N 10,06; found: C 72.18, H 6.27, N 10.34.

Methyl 1-(2-cyano-5-methoxyphenyl)-1*H*-pyrrole-2-carboxylate (24). To a stirred solution of methyl 1*H*-pyrrole-2-carboxylate (1.0 g, 8.00 mmol) in dry DMF (25.0 mL), Cs_2CO_3 (13.0 g, 40.00 mmol) and **23** (1.5 g, 9.60 mmol) were added and the reaction was stirred at 50 °C under N_2 atmosphere for 12 h. Solvent was removed under reduced pressure and the crude was taken up with a saturated solution of NH_4Cl. The aqueous phase was extracted with DCM (3 x 25.0 mL) and the combined organic layers were dried over Na_2SO_4, filtered, and evaporated. The crude was purified by means of chromatography on silica gel (ethyl acetate/petroleum ether 1:6) to afford compound title compound (30% yield) as a colourless solid. ^{1}H NMR (300 MHz, $CDCl_3$) δ 3.74 (s, 3H), 3.87 (s, 3H), 6.37 (dd, *J* = 3.8, 2.9 Hz, 1H), 6.90 (d, *J* = 2.5 Hz, 1H), 6.94 (q, *J* = 2.6 Hz, 1H), 7.00 (dd, *J* = 8.7, 2.5 Hz, 1H), 7.13 (dd, *J* = 3.9, 1.7 Hz, 1H), 7.64 (d, *J* = 8.7 Hz, 1H). ESI-MS *m/z* 257 $[M + H]^+$, 279 $[M + Na]^+$.

9-Hydroxy-5,6-dihydro-4*H*-benzo[*f*]pyrrolo[1,2-*a*][1,4]diazepin-4-one (25). Starting from **24** (600 mg, 2.34 mmol), *9-methoxy-5,6-dihydro-4H-benzo[f]pyrrolo[1,2-a][1,4]diazepin-4-one* was obtained following the same procedure reported for **22**. The crude was purified by means of chromatography on silica gel (ethyl acetate/petroleum ether 1:1) to afford compound *9-methoxy-5,6-dihydro-4H-benzo[f]pyrrolo[1,2-a][1,4]diazepin-4-one* (71% yield) as a colourless solid. ^{1}H NMR (300 MHz, $CDCl_3$) δ 3.80 (s, 3H), 4.14 (s, 2H), 6.36-6.47 (m, 1H), 6.75 (dd, *J* = 8.3, 1.9 Hz, 1H), 6.83 (d, *J* = 2.3 Hz, 1H), 7.07-7.15 (m, 1H), 7.15-7.24 (m, 2H), 8.23 (br s, 1H). ESI-MS *m/z* 229 $[M + H]^+$, 251 $[M + Na]^+$.

Starting from *9-methoxy-5,6-dihydro-4H-benzo[f]pyrrolo[1,2-a][1,4]diazepin-4-one* (380 mg, 1.66 mmol), the title compound was obtained following the same procedure reported for **14**. The crude was purified by means of chromatography on silica gel (EtOAc) to afford title compound (50% yield) as a colourless solid. ^{1}H NMR (300 MHz, CD_3OD) δ 4.08 (s, 2H), 6.42 (t, *J* = 3.1 Hz, 1H), 6.74 (dd, *J* = 8.2, 2.1 Hz, 1H), 6.85 (d, *J* = 2.2 Hz, 1H), 7.02 (dd, *J* = 3.8, 1.1 Hz, 1H), 7.21 (d, *J* = 8.2 Hz, 1H), 7.32-7.40 (m, 1H). ESI-MS *m/z* 215 $[M + H]^+$, 237 $[M + Na]^+$.

4-Oxo-5,6-dihydro-4*H*-benzo[*f*]pyrrolo[1,2-*a*][1,4]diazepin-9-yl-(6-phenylhexyl)carbamate (5i). Starting from **25** (10 mg, 0.05 mmol) and 6-phenylhexyl isocyanate **7b** (13 mg, 0.06 mmol), the title compound was obtained following the same procedure reported for **5a**. The crude was purified by means of chromatography on silica gel (MeOH/DCM 1:20) to afford the title compound (52% yield) as a colourless solid. ^{1}H NMR (300 MHz, $CDCl_3$) δ 1.33-1.44 (m, 4H), 1.48-1.71 (m, 4H), 2.61 (t, *J* = 5.1 Hz, 2H), 3.24 (q, *J* = 6.6 Hz, 2H), 4.17 (br d, 2H), 5.25 (t, *J* = 4.2 Hz, 1H), 6.42 (t, *J* = 3.3 Hz, 1H), 7.01 (dd, *J* = 8.2, 2.1 Hz, 1H), 7.07-7.22 (m, 6H), 7.22-7.33 (m, 3H), 7.45 (t, *J* = 5.2 Hz, 1H). ESI-MS *m/z* 375 $[M + H]^+$; HRMS (ESI) *m/z* calcd for $C_{25}H_{28}N_3O_3^+$: 418,2125, found 418,2117 $[M + H]^+$; calcd for: $C_{25}H_{27}N_3NaO_3^+$: 440,1945 found 440,1936 $[M + Na]^+$, calcd for $C_{50}H_{55}N_6O_6^+$: 835,4178 found 835,4168 $[2M + H]^+$. Elemental analysis calcd (%) for $C_{25}H_{27}N_3O_3$: C 71.92, H 6.52, N 10.06; found C 72.11, H 6.35, N 10.20.

4-Oxo-5,6-dihydro-4*H*-benzo[*f*]pyrrolo[1,2-*a*][1,4]diazepin-9-yl-(2-(2-phenoxyethoxy)ethyl) carbamate (5j). Starting from **25** (10 mg, 0.05 mmol) and isocyanate **26a** (13 mg, 0.06 mmol), the title compound was obtained following the same procedure reported for **5a**. The crude was purified by means of chromatography on silica gel (MeOH/DCM 1:20) to afford title compound (55% yield) as a colourless solid. ^{1}H NMR (300 MHz, $CDCl_3$) δ 3.46-3.54 (m, 2H), 3.71 (t, *J* = 4.8 Hz, 2H), 3.80-3.92 (m, 2H), 4.07-4.25 (m, 4H), 5.66 (t, *J* = 4.5 Hz, 1H), 6.43 (t, *J* = 3.3 Hz, 1H), 6.89-6.99 (m, 3H), 7.00-7.17 (m, 4H), 7.20 (s, 1H), 7.23-7.34 (m, 3H); ^{13}C NMR (75 MHz, $CDCl_3$) δ 41.3, 43.2, 67.5, 69.9, 70.1, 111.2, 114.8, 116.8, 118.7, 119.9, 121.4, 125.1, 128.7, 129.0, 129.3, 129.8, 140.0, 151.7, 154.4, 158.8. ESI-MS *m/z* 422 $[M + H]^+$ (100). Elemental analysis calcd (%) for $C_{23}H_{23}N_3O_5$: C 65.55 , H 5.50, N 9.97; found: C 65.23, H 5.29, N 9.76.

4-Oxo-5,6-dihydro-4*H*-benzo[*f*]pyrrolo[1,2-*a*][1,4]diazepin-9-yl-(2-(2-(2-fluorophenoxy)ethoxy)ethyl) carbamate (5k). Starting from **25** (10 mg, 0.05 mmol) and isocyanate **26b** (14 mg, 0.06 mmol), the title compound was obtained following the same procedure reported for **5a**. The crude was purified by means of chromatography on silica gel (MeOH/DCM 1:20) to afford title compound (47% yield) as a colourless solid. ^{1}H NMR (300 MHz, $CDCl_3$) δ 3.49 (q, *J* = 10.3 Hz, 2H), 3.71 (t, *J* = 5.0 Hz, 2H), 3.84-3.93 (m, 2H), 4.14-4.26 (m, 4H), 5.65 (t, *J* = 5.6 Hz, 1H), 6.42 (dd, *J* = 3.8, 2.9 Hz, 1H), 6.86-6.96 (m, 1H), 6.96-7.11 (m, 4H), 7.11-7.17 (m, 3H), 7.17-7.23 (m, 1H), 7.28 (s, 1H); ^{13}C NMR (75 MHz, $CDCl_3$) δ 41.3, 43.2, 69.3, 69.7, 70.2, 111.3, 115.8, 116.60 (d, $J_{C\text{-}F}$ = 18.2 Hz), 116.9, 118.9, 120.0, 121.98 (d, $J_{C\text{-}F}$ = 6.8 Hz), 124.57 (d, $J_{C\text{-}F}$ = 3.9 Hz), 125.3, 128.8, 129.3, 140.0, 146.93 (d, $J_{C\text{-}F}$ = 10.6 Hz), 151.7, 153.13 (d, $J_{C\text{-}F}$ = 245.6 Hz), 154.4, 164.2. ESI-MS *m/z* 440 $[M + H]^+$. Elemental analysis calcd (%) for $C_{23}H_{22}FN_3O_5$: C 62.86, H 5.05, N 9.56; found: C 63.12, H 5.18, N 9.47.

4-Oxo-5,6-dihydro-4*H*-benzo[*f*]pyrrolo[1,2-*a*][1,4]diazepin-9-yl-(2-(2-(4-fluorophenoxy)ethoxy)ethyl) carbamate (5l). Starting from **25** (10 mg, 0.05 mmol) and isocyanate **26c** (14 mg, 0.06 mmol), the title compound was obtained following the same procedure reported for **5a**. The crude was purified by means of chromatography on silica gel (MeOH/DCM 1:20) to afford title compound (43% yield) as a colourless solid. ^{1}H NMR (300 MHz, $CDCl_3$) δ 3.50 (q, *J* = 5.2 Hz, 2H), 3.70 (t, *J* = 5.0 Hz, 2H), 3.82-3.89 (m, 2H), 4.07-4.14 (m, 2H), 4.20 (br d, *J* = 3.4 Hz, 2H), 5.61 (t, *J* = 5.7 Hz, 1H), 6.43 (t, *J* = 3.8 Hz, 1H), 6.81-6.92 (m, 2H), 6.92-7.11 (m, 4H), 7.11-7.17 (m, 2H), 7.17-7.22 (m, 1H), 7.26-7.31 (m, 1H); ^{13}C NMR (75 MHz, $CDCl_3$) δ 41.3, 43.1, 68.2, 69.9, 70.1, 111.3, 115.9 (d, $J_{C\text{-}F}$ = 8.0 Hz), 116.1 (d, $J_{C\text{-}F}$ = 23.1 Hz), 116.8, 118.8, 119.9, 125.2, 128.6, 128.9, 129.2, 140.0, 151.6, 154.3, 155.0 (d, $J_{C\text{-}F}$ = 2.1 Hz), 157.6 (d, $J_{C\text{-}F}$ = 238.7 Hz), 164.2. ESI-MS *m/z* 440 $[M + H]^+$. Elemental analysis calcd (%) for $C_{23}H_{22}FN_3O_5$: C 62.86, H 5.05, N 9.56; found: C 62.67, H 4.78, N 9.21.

Molecular Docking Studies

a) Ligand preparation

Three-dimensional structures of all compounds in this study were built by means of Maestro (Maestro, version 9.3, Schrödinger, LLC, New York, NY, 2012). Molecular energy minimizations were performed by means of MacroModel (MacroModel, version 9.9, Schrödinger, LLC, New York, NY, 2012) using the Optimized Potentials for Liquid Simulations-all atom (OPLS-AA) force field 2005.[41] The solvent effects were simulated using the analytical Generalized-Born/Surface-Area (GB/SA) model,[42] and no cutoff for nonbonded interactions was selected. Polak-Ribiere conjugate gradient (PRCG) method with 1000 maximum iterations and 0.001 gradient convergence threshold was employed. All compounds reported in this paper were treated by LigPrep application (LigPrep, version 2.5, Schrödinger, LLC, New York, NY, 2012), implemented in Maestro suite 2011, generating the most probable ionization state of any possible enantiomers and tautomers at cellular pH value (7 ± 0.5) and also for avoiding potential error in the structures.

b) Protein preparation

The three-dimensional structure of FAAH (PDB ID: 3PPM[43]) was taken from PDB and imported into Schrödinger Maestro molecular modeling environment. Water molecules and compounds used for the crystallization were removed from the available experimental structure. The obtained enzyme was submitted to protein preparation

wizard implemented in Maestro suite 2012. This protocol through a series of computational steps, allowed us to obtain a reasonable starting structure of the protein for molecular docking calculations by a series of computational steps. In particular, we performed three steps to (1) add hydrogens, (2) optimize the orientation of hydroxyl groups, Asn, and Gln, and the protonation state of His, and (3) perform a constrained refinement with the impref utility, setting the max RMSD of 0.30. The impref utility consists of a cycles of energy minimization based on the impact molecular mechanics engine and on the OPLS_2005 force field.[41]

c) Molecular Docking

Molecular docking was carried out using the Schrödinger suite 2012 by applying the IFD protocol (Schrödinger Suite 2012 Induced Fit Docking protocol; Glide version 5.8, Schrödinger, LLC, New York, NY, 2012; Prime version 3.1, Schrödinger, LLC, New York, NY, 2012). This procedure induces conformational changes in the binding site to accommodate the ligand and exhaustively identify possible binding modes and associated conformational changes by side-chain sampling and backbone minimization. The protein and the ligands used were prepared as reported in the previous paragraphs. The boxes for docking calculation were built taking into account the centroid of the co-crystallized ligand for FAAH enzyme. Complexes within 30.0 kcal/mol of minimum energy structure were taken forward for redocking. The Glide redocking stage was performed by XP (Extra Precision) methods. The calculations were performed using default IFD protocol parameters. No hydrogen bonding or other constraints were used. The choice of IFD coupled to XP was done after the assessment of two docking protocols (IFD-SP and IFD-XP). From the computational outputs we observed that IFD-XP was able to correctly accommodate the co-crystallized ligands, belonging to the FAAH crystal structures 3PPM, 3QJ9 and 2VYA, with lower RMSD than IFD-SP (data not shown).

Enzymatic assays

FAAH and MAGL activities were detected in cells as previously described.[44-45] In particular, AEA hydrolysis was measured by incubating samples with the 10,000x g membrane fraction of rat brain (70 µg/sample) and synthetic N-arachidonoyl-[^{14}C]-ethanolamine (110mCi/mmol, ARC St. Louis, MO, USA) properly diluted with AEA (Tocris Bioscience, Avonmouth, Bristol, UK) in Tris–HCl 50 mM, at pH 9.00–10.00 at 37 °C for 30 min. After incubation, the amount of [^{14}C]-ethanolamine produced was measured by scintillation counting of the aqueous phase after extraction of the incubation mixture with 2 volumes of $CHCl_3$/MeOH 1:1 (by vol.). 2-AG hydrolysis was measured by incubating the 10,000xg cytosolic fraction of COS-7 cells (100 µg/sample), which contains high levels of MAGL, and synthetic 2-arachidonoyl-[3H]-glycerol (40 Ci/mmol, ARC St. Louis, MO, USA) properly diluted with 2-AG (Cayman Chemicals, Ann Arbor, MI, USA) in Tris–HCl 50 mM, at pH 7.0 at 37°C for 20 min. After incubation, the amount of [^{3}H]-glycerol produced was measured by scintillation counting of the aqueous phase after extraction of the incubation mixture with 2 volumes of $CHCl_3$/MeOH 1:1 (by vol.). All data are expressed as means ± SD of three separate experiments of the concentration exerting 50% inhibition of [^{14}C]-AEA hydrolysis (IC_{50}) calculated by fitting sigmoidal concentration response curves by GraphPad.

Competition Binding Assay

Membranes from HEK-293 cells over-expressing the respective human recombinant CB1 receptor (Bmax= 2.5 pmol/mg protein) and human recombinant CB2 receptor (Bmax= 4.7 pmol/mg protein) were incubated with [^{3}H]-CP-55,940 (0.14nM/*K*d=0.18nM and 0.084nM/*K*d=0.31nM, respectively for CB1 and CB2 receptor) as the high affinity ligand. Competition curves were performed as previously reported[46] by displacing [^{3}H]-CP-55,940 with increasing concentration of compounds (0.1–50 µM). Nonspecific binding was defined by 10 µM of WIN55,212-2 as the heterologous competitor (*K*i values 9.2 nM and 2.1 nM respectively for CB1 and CB2 receptor). IC_{50} values were determined for compounds showing >50% displacement at 10 µM. All compounds were tested following the procedure described by the manufacturer (Perkin Elmer, Italy). Displacement curves were generated by incubating drugs with [^{3}H]-CP-55,940 for 90 minutes at 30 ºC. Ki values were calculated by applying the Cheng-Prusoff equation to the IC_{50} values (obtained by GraphPad) for the displacement of the bound radioligand by increasing concentrations of the test compound. Data represent mean values of three separate experiments performed in duplicate and are expressed as the average of *K*i ± SD.

Cellular *in vitro* study

a) Cell culture and treatments

IMR32 cells line (obtained from American Type Culture Collection, ATCC), were cultured in EMEM medium supplemented with 10% fetal bovine serum (Lonza, Milan, Italy) supplemented with 10% fetal bovine serum (FBS, EuroClone, Milan, Italy), 1% of L-glutammine (Lonza, Milan, Italy) and 1% of penicillin/streptomycin antibiotics (Lonza, Milan, Italy) at 37 °C in 5% CO_2. The different formulations (**3**, **5h**, and **5i**) were dissolved in DMSO as stock solutions at the final concentration of 10 mM. Stock solutions were then diluted with cell culture medium, EMEM with Earle's Balanced Salt Solution, to obtain an intermediate dose solution (100 µM), to be used for the used dilutions (50 µM, 10 µM, 5 µM, 1 µM, 0.5 µM and 0.1 µM). Control vehicle was represented by DMSO ranging from 0.5% to 0.001%.

b) Cytotoxicity determination

IMR32 cells were seeded 100,000 cells/well in 96-wells plate and were grown to confluence, then were treated with the tested substances in EMEM medium supplemented with 10% fetal bovine serum. The effects of tested compounds on cellular morphology were checked after 24 h using a built-in camera in an inverted Nikon Eclipse microscope (20X magnification). Cytotoxicity was determined by LDH release in the media, measured by enzymatic assay: in the first step NADþ is reduced to NADH/Hþ by LDH-catalyzed conversion of lactate to pyruvate; in the second step the catalyst (diaphorase) transfers H/Hþ from NADH/Hþ to tetrazolium salt which is reduced to formazan. For total release of intracellular LDH (positive control of 100% cell death), a triplicate set of IMR32 cells were treated with 1% Triton X-100 for 30 min at 37 °C, according to the manufacturer's protocol (Roche, Mannheim, Germany). The amount of LDH in the supernatant was determined and calculated according to kit instructions. The amount of LDH release in each sample was determined by measuring the absorbance at 490 nm using a microplate spectrophotometer. All tests were performed at least in triplicate. The absorbance measured from three wells was averaged, and the percentage of LDH released was calculated as arbitrary unit of change relative to 1% Triton X-100 treated cells.

c) Nuclear proteins extraction

For nuclear extracts, IMR32 cells were seeded in 100 mm petri (3 x 10^6 cells). After treatments with different compounds, cells were detached, washed with ice-cold PBS 1X and cell pellets were resuspended in hypotonic buffer containing 10 mmol/L HEPES (pH 7.9), 10 mmol/L KCl, 1.5 mmol/L $MgCl_2$, 0.3% Nonidet P-40, 0.5 mmol/L dithithreitiol, 0.5 mmol/L phenylmethylsulphonyl fluoride and protease and phosphatase inhibitor cocktails. The lysates were incubated for 15 minutes on ice with intermitted mixing and then centrifuged at 24500 x g for 15 min at 4 °C. The supernatant containing the cytosolic proteins was removed and pellet containing the nuclei were resuspended in extraction buffer containing 20 mmol/L HEPES (pH 7.9), 0,6 mol/L KCl, 1.5 mmol/L $MgCl_2$, 20% glycerol, 0.5 mmol/L phenylmethylsulphonyl fluoride and protease and phosphatase inhibitor cocktails and then incubated for 30 minutes on

ice with intermitted mixing. Samples were centrifuged at 21100 x g for 15 minutes to obtain supernatants containing nuclear fractions. Protein concentration was determined by Bradford analysis (Biorad protein assay; Biorad, Milan, Italy).

d) Western blot analysis

After protein quantification, 60 µg boiled proteins were loaded into 10% sodium dodecyl sulphatepolyacrylamide electrophoresis gels and separated by molecular size. Gels were electro-blotted onto nitrocellulose membranes and then blocked for 90 minutes in Tris-buffered saline, pH 7.5, containing 0.5% Tween 20 and 5% (w/v) skim milk powder. Membranes were incubated overnight at 4°C with the appropriate primary antibody: anti-NF-kB, p65 subunit, diluted 1:1000 (Millipore, Billerica, Massachusetts). The membranes were finally incubated with the peroxidase-conjugated secondary anti-Rabbit antibody (1:5000) for 1 h. The bound antibodies were detected by chemiluminescence (Biorad, Milan, Italy). β-Actin was used as loading control. Images of the bands were digitized using an Epson Stylus SX405 scanner and the densitometry analysis was performed using Image-J software.

e) Statistical analysis

For each of the variables tested, two-way analysis of variance (ANOVA) was used. A significant result was indicated by a p value < 0.05. All the results are expressed as mean ± SD of triplicate determinations obtained in 3 independent experiments. Data were analyzed using the software GraphPad Prism 4.0 (GraphPad Software, Inc., La Jolla, CA).

Pharmacological *in vivo* study

a) Animals

Male CD-1 albino mice (Envigo, Varese, Italy) weighing approximately 22–25 g at the beginning of the experimental procedure, were used. Animals were housed in CeSAL (Centro Stabulazione Animali da Laboratorio, University of Florence) and used at least 1 week after their arrival. Ten mice were housed per cage (size 26 × 41 cm); animals were fed a standard laboratory diet and tap water *ad libitum*, and kept at 23 ± 1 °C with a 12 h light/dark cycle, light at 7 a.m. All animal manipulations were carried out according to the Directive 2010/63/EU of the European parliament and of the European Union council (22 September 2010) on the protection of animals used for scientific purposes. The ethical policy of the University of Florence complies with the Guide for the Care and Use of Laboratory Animals of the US National Institutes of Health (NIH Publication No. 85-23, revised 1996; University of Florence assurance number: A5278-01). Formal approval to conduct the experiments described was obtained from the Animal Subjects Review Board of the University of Florence. Experiments involving animals have been reported according to ARRIVE guidelines. All efforts were made to minimize animal suffering and to reduce the number of animals used.

b) Oxaliplatin-induced neuropathic pain model and compound administration.

Oxaliplatin (2.4 mg kg^{-1}) was dissolved in 5% glucose solution and i.p. administered for 5 consecutive days every week for 2 weeks.[40] On day 14, compounds **3**, **5h** and **5i** were administered p.o.[47-48] using 1% carboxymethylcellulose (CMC) as vehicle.

c) Cold plate test

The animals were placed in a stainless steel box (12 cm × 20 cm × 10 cm) with a cold plate as floor. The temperature of the cold plate was kept constant at 4 °C ± 1 °C. Pain-related behavior (licking of the hind paw) was observed and the time (s) of the first sign was recorded. The cut-off time of the latency of paw lifting or licking was set at 60 s.[49] Measurements were performed before and 15, 30, 45 and 60 min after compound administration.

d) Statistical analysis

Behavioural measurements were performed on 12 mice for each treatment carried out in 2 different experimental sets. Results were expressed as mean ± S.E.M. The analysis of variance of behavioural data was performed by one way ANOVA, a Bonferroni's significant difference procedure was used as post-hoc comparison. *P* values of less than 0.05 or 0.01 were considered significant. Investigators were blind to all experimental procedures. Data were analysed using the "Origin 9" software (OriginLab, Northampton, USA).

Acknowledgements

The authors wish to thank Miur PRIN 20088SPEFN_005.

Keywords: endocannabinoid system, fatty acid amide hydrolase, covalent inhibitors, neuropathic pain, serine hydrolase

Abbreviations. FAAH, fatty acid amide hydrolase; ECs, endocannabinoids; CBR, cannabinoid receptor; FAEs, fatty acid ethanolamides; AEA, anandamide; MAGL, monoacylglycerol lipase; CNS, central nervous system; SAR, structure-activity relationship; THF, tetrahydrofuran; TEA, triethylamine; DMF, dimethylformamide; 1,2-DCE, 1,2-dichloroethane; DCM, dichloromethane; DMSO, dimethylsulfoxide; CMC, carboxymethylcellulose; PDB, Protein Data Bank.

Received: ((will be filled in by the editorial staff))
Published online: ((will be filled in by the editorial staff))

References:

[1] M. P. Patricelli, B. F. Cravatt, *Biochemistry* **1999**, *38*, 14125-14130.
[2] D. K. Giang, B. F. Cravatt, *Proc Natl Acad Sci U S A* **1997**, *94*, 2238-2242.
[3] M. P. Patricelli, M. A. Lovato, B. F. Cravatt, *Biochemistry* **1999**, *38*, 9804-9812.
[4] K. Tsuboi, Y. X. Sun, Y. Okamoto, N. Araki, T. Tonai, N. Ueda, *J Biol Chem* **2005**, *280*, 11082-11092.
[5] M. Karlsson, J. A. Contreras, U. Hellman, H. Tornqvist, C. Holm, *J Biol Chem* **1997**, *272*, 27218-27223.
[6] W. A. Devane, L. Hanus, A. Breuer, R. G. Pertwee, L. A. Stevenson, G. Griffin, D. Gibson, A. Mandelbaum, A. Etinger, R. Mechoulam, *Science* **1992**, *258*, 1946-1949.
[7] R. Mechoulam, S. Ben-Shabat, L. Hanus, M. Ligumsky, N. E. Kaminski, A. R. Schatz, A. Gopher, S. Almog, B. R. Martin, D. R. Compton, et al., *Biochem Pharmacol* **1995**, *50*, 83-90.
[8] J. Zias, H. Stark, J. Sellgman, R. Levy, E. Werker, A. Breuer, R. Mechoulam, *Nature* **1993**, *363*, 215.
[9] A. H. Lichtman, C. C. Shelton, T. Advani, B. F. Cravatt, *Pain* **2004**, *109*, 319-327.
[10] F. Massa, G. Marsicano, H. Hermann, A. Cannich, K. Monory, B. F. Cravatt, G. L. Ferri, A. Sibaev, M. Storr, B. Lutz, *J Clin Invest* **2004**, *113*, 1202-1209.
[11] S. Huitron-Resendiz, M. Sanchez-Alavez, D. N. Wills, B. F. Cravatt, S. J. Henriksen, *Sleep* **2004**, *27*, 857-865.
[12] S. A. Varvel, L. E. Wise, F. Niyuhire, B. F. Cravatt, A. H. Lichtman, *Neuropsychopharmacology* **2007**, *32*, 1032-1041.
[13] M. Seierstad, J. G. Breitenbucher, *J Med Chem* **2008**, *51*, 7327-7343.
[14] Y. Miyake, J. J. Keusch, L. Wang, M. Saito, D. Hess, X. Wang, B. J. Melancon, P. Helquist, H. Gut, P. Matthias, *Nat Chem Biol* **2016**, *12*, 748-754.
[15] A. C. M. van Esbroeck, A. P. A. Janssen, A. B. Cognetta, 3rd, D. Ogasawara, G. Shpak, M. van der Kroeg, V. Kantae, M. P. Baggelaar, F. M. S. de Vrij, H. Deng, M. Allara, F. Fezza, Z. Lin, T. van der Wel, M. Soethoudt, E. D. Mock, H. den Dulk, I. L. Baak, B. I. Florea, G. Hendriks, L. De Petrocellis, H. S. Overkleeft, T. Hankemeier, C. I. De Zeeuw, V. Di Marzo, M. Maccarrone, B. F. Cravatt, S. A. Kushner, M. van der Stelt, *Science* **2017**, *356*, 1084-1087.
[16] M. Duenas, B. Ojeda, A. Salazar, J. A. Mico, I. Failde, *J Pain Res* **2016**, *9*, 457-467.
[17] B. K. Lau, C. W. Vaughan, *Front Pharmacol* **2014**, *5*, 28.
[18] M. H. Bracey, M. A. Hanson, K. R. Masuda, R. C. Stevens, B. F. Cravatt, *Science* **2002**, *298*, 1793-1796.
[19] G. Tarzia, A. Duranti, A. Tontini, G. Piersanti, M. Mor, S. Rivara, P. V. Plazzi, C. Park, S. Kathuria, D. Piomelli, *J Med Chem* **2003**, *46*, 2352-2360.

[20] J. P. Alexander, B. F. Cravatt, *Chem Biol* **2005**, *12*, 1179-1187.
[21] D. L. Boger, H. Miyauchi, W. Du, C. Hardouin, R. A. Fecik, H. Cheng, I. Hwang, M. P. Hedrick, D. Leung, O. Acevedo, C. R. Guimaraes, W. L. Jorgensen, B. F. Cravatt, *J Med Chem* **2005**, *48*, 1849-1856.
[22] S. Butini, M. Brindisi, S. Gemma, P. Minetti, W. Cabri, G. Gallo, S. Vincenti, E. Talamonti, F. Borsini, A. Caprioli, M. A. Stasi, S. Di Serio, S. Ros, G. Borrelli, S. Maramai, F. Fezza, G. Campiani, M. Maccarrone, *J Med Chem* **2012**, *55*, 6898-6915.
[23] S. Butini, S. Gemma, M. Brindisi, S. Maramai, P. Minetti, D. Celona, R. Napolitano, F. Borsini, W. Cabri, F. Fezza, L. Merlini, S. Dallavalle, G. Campiani, M. Maccarrone, *Bioorg Med Chem Lett* **2013**, *23*, 492-495.
[24] M. Brindisi, S. Maramai, S. Gemma, S. Brogi, A. Grillo, L. Di Cesare Mannelli, E. Gabellieri, S. Lamponi, S. Saponara, B. Gorelli, D. Tedesco, T. Bonfiglio, C. Landry, K. M. Jung, A. Armirotti, L. Luongo, A. Ligresti, F. Piscitelli, C. Bertucci, M. P. Dehouck, G. Campiani, S. Maione, C. Ghelardini, A. Pittaluga, D. Piomelli, V. Di Marzo, S. Butini, *J Med Chem* **2016**, *59*, 2612-2632.
[25] M. Brindisi, S. Brogi, S. Maramai, A. Grillo, G. Borrelli, S. Butini, E. Novellino, M. Allara, A. Ligresti, G. Campiani, V. Di Marzo, S. Gemma, *RSC Adv* **2016**, *6*, 64651-64664.
[26] J. Lim, M. Igarashi, K. M. Jung, S. Butini, G. Campiani, D. Piomelli, *Neuropsychopharmacology* **2016**, *41*, 1329-1339.
[27] R. Colangeli, M. Pierucci, A. Benigno, G. Campiani, S. Butini, G. Di Giovanni, *Sci Rep* **2017**, *7*, 11152.
[28] G. Campiani, A. Cappelli, V. Nacci, M. Anzini, S. Vomero, M. Hamon, A. Cagnotto, C. Fracasso, C. Uboldi, S. Caccia, S. Consolo, T. Mennini, *J Med Chem* **1997**, *40*, 3670-3678.
[29] S. Butini, R. Budriesi, M. Hamon, E. Morelli, S. Gemma, M. Brindisi, G. Borrelli, E. Novellino, I. Fiorini, P. Ioan, A. Chiarini, A. Cagnotto, T. Mennini, C. Fracasso, S. Caccia, G. Campiani, *J Med Chem* **2009**, *52*, 6946-6950.
[30] E. Morelli, S. Gemma, R. Budriesi, G. Campiani, E. Novellino, C. Fattorusso, B. Catalanotti, S. S. Coccone, S. Ros, G. Borrelli, M. Persico, I. Fiorini, V. Nacci, P. Ioan, A. Chiarini, M. Hamon, A. Cagnotto, T. Mennini, C. Fracasso, M. Colovic, S. Caccia, S. Butini, *J Med Chem* **2009**, *52*, 3548-3562.
[31] A. Cappelli, S. Butini, A. Brizzi, S. Gemma, S. Valenti, G. Giuliani, M. Anzini, L. Mennuni, G. Campiani, V. Brizzi, S. Vomero, *Curr Top Med Chem* **2010**, *10*, 504-526.
[32] M. Brindisi, S. Butini, S. Franceschini, S. Brogi, F. Trotta, S. Ros, A. Cagnotto, M. Salmona, A. Casagni, M. Andreassi, S. Saponara, B. Gorelli, P. Weikop, J. D. Mikkelsen, J. Scheel-Kruger, K. Sandager-Nielsen, E. Novellino, G. Campiani, S. Gemma, *J Med Chem* **2014**, *57*, 9578-9597.
[33] S. Butini, M. Brindisi, S. Brogi, S. Maramai, E. Guarino, A. Panico, A. Saxena, V. Chauhan, R. Colombo, L. Verga, E. De Lorenzi, M. Bartolini, V. Andrisano, E. Novellino, G. Campiani, S. Gemma, *ACS Med Chem Lett* **2013**, *4*, 1178-1182.
[34] M. Chioua, M. Perez, O. M. Bautista-Aguilera, M. Yanez, M. G. Lopez, A. Romero, R. Cacabelos, R. P. de la Bellacasa, S. Brogi, S. Butini, J. I. Borrell, J. Marco-Contelles, *Mini Rev Med Chem* **2015**, *15*, 648-658.
[35] M. Y. Wu, G. Esteban, S. Brogi, M. Shionoya, L. Wang, G. Campiani, M. Unzeta, T. Inokuchi, S. Butini, J. Marco-Contelles, *Eur J Med Chem* **2016**, *121*, 864-879.
[36] C. Carrasco, M. Naziroglu, A. B. Rodriguez, J. A. Pariente, *Front Physiol* **2018**, *9*, 95.
[37] L. Di Cesare Mannelli, M. Zanardelli, P. Failli, C. Ghelardini, *J Pain* **2012**, *13*, 276-284.
[38] S. Brogi, A. Ramunno, L. Savi, G. Chemi, G. Alfano, A. Pecorelli, E. Pambianchi, P. Galatello, G. Compagnoni, F. Focher, G. Biamonti, G. Valacchi, S. Butini, S. Gemma, G. Campiani, M. Brindisi, *Eur J Med Chem* **2017**, *138*, 438-457.
[39] L. Di Cesare Mannelli, A. Pacini, L. Bonaccini, M. Zanardelli, T. Mello, C. Ghelardini, *J Pain* **2013**, *14*, 1585-1600.
[40] G. Cavaletti, G. Tredici, M. G. Petruccioli, E. Donde, P. Tredici, P. Marmiroli, C. Minoia, A. Ronchi, M. Bayssas, G. G. Etienne, *Eur J Cancer* **2001**, *37*, 2457-2463.
[41] W. L. Jorgensen, D. S. Maxwell, J. TiradoRives, *J Am Chem Soc* **1996**, *118*, 11225-11236.
[42] W. C. Still, A. Tempczyk, R. C. Hawley, T. Hendrickson, *J Am Chem Soc* **1990**, *112*, 6127-6129.
[43] M. Mileni, J. Garfunkle, C. Ezzili, B. F. Cravatt, R. C. Stevens, D. L. Boger, *J Am Chem Soc* **2011**, *133*, 4092-4100.
[44] S. Montanari, L. Scalvini, M. Bartolini, F. Belluti, S. Gobbi, V. Andrisano, A. Ligresti, V. Di Marzo, S. Rivara, M. Mor, A. Bisi, A. Rampa, *J Med Chem* **2016**, *59*, 6387-6406.
[45] G. Ortar, T. Bisogno, A. Ligresti, E. Morera, M. Nalli, V. Di Marzo, *J Med Chem* **2008**, *51*, 6970-6979.
[46] N. A. Osman, A. Ligresti, C. D. Klein, M. Allara, A. Rabbito, V. Di Marzo, K. A. Abouzid, A. H. Abadi, *Eur J Med Chem* **2016**, *122*, 619-634.
[47] C. Battilocchio, G. Poce, S. Alfonso, G. C. Porretta, S. Consalvi, L. Sautebin, S. Pace, A. Rossi, C. Ghelardini, L. Di Cesare Mannelli, S. Schenone, A. Giordani, L. Di Francesco, P. Patrignani, M. Biava, *Bioorg Med Chem* **2013**, *21*, 3695-3701.
[48] M. Anzini, S. Valenti, C. Braile, A. Cappelli, S. Vomero, S. Alcaro, F. Ortuso, L. Marinelli, V. Limongelli, E. Novellino, L. Betti, G. Giannaccini, A. Lucacchini, S. Daniele, C. Martini, C. Ghelardini, L. Di Cesare Mannelli, G. Giorgi, M. P. Mascia, G. Biggio, *J Med Chem* **2011**, *54*, 5694-5711.
[49] L. Di Cesare Mannelli, A. Pacini, F. Corti, S. Boccella, L. Luongo, E. Esposito, S. Cuzzocrea, S. Maione, A. Calignano, C. Ghelardini, *PLoS One* **2015**, *10*, e0128080.

Entry for the Table of Contents

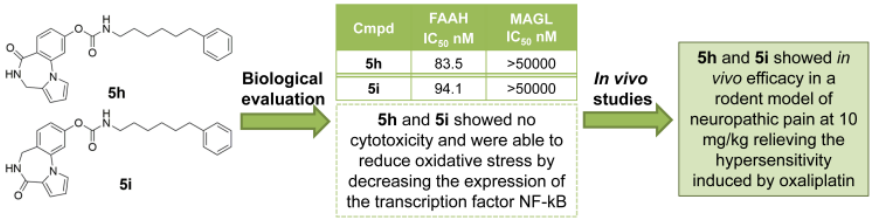

By rational design, aiming at discovering selective FAAH inhibitors to exploit the therapeutic effects against neuropathic pain, we develop a series of compounds characterized by a functionalized tricyclic scaffolds. The most potent non toxic FAAH inhibitors **5h** and **5i** reduced oxidative stress by decreasing the expression of NF-kB, showed efficacy in a mice model of neuropathic pain relieving the hypersensitivity induced by oxaliplatin.